arXiv:2511.17441v3 [cs.RO] 13 Apr 2026

RoboCOIN: An Open-Sourced Bimanual Robotic Data COllection for INtegrated Manipulation

Shihan Wu[1,2*†], Xuecheng Liu[1*†], Shaoxuan Xie[1*†], Pengwei Wang[1*], Xinghang Li[1*], Bowen Yang[3], Zhe Li[3], Kai Zhu[3], Hongyu Wu[1,4], Yiheng Liu[1,4], Zhaoye Long[1,5], Runtian Xu[1,4], Yue Wang[1], Chong Liu[1,4], Dihan Wang[1,4], Ziqiang Ni[1], Xiang Yang[1], You Liu[1], Ruoxuan Feng[1,6], Lei Zhang[1,7], Denghang Huang[1,8], Chenghao Jin[1,9], Anlan Yin[1,10], Xinlong Wang[1], Zhenguo Sun[1], Junkai Zhao[1], Mengfei Du[1], Mingyu Cao[1], Xiansheng Chen[1], Hongyang Cheng[1], Xiaojie Zhang[1], Yankai Fu[1,11], Ning Chen[1,11], Cheng Chi[1], Sixiang Chen[1,11], Huaihai Lyu[1,7], Xiaoshuai Hao[1], Yequan Wang[1], Bo Lei[1], Dong Liu[1], Xi Yang[1], Yance Jiao[1], Tengfei Pan[1], Yunyan Zhang[1], Songjing Wang[1], Ziqian Zhang[1], Xu Liu[1], Ji Zhang[12], Caowei Meng[13], Zhizheng Zhang[13,1], Jiyang Gao[14], Song Wang[15], Xiaokun Leng[15], Zhiqiang Xie[16], Zhenzhen Zhou[16], Peng Huang[17], Wu Yang[17], Yandong Guo[18], Yichao Zhu[18], Suibing Zheng[19], Hao Cheng[20], Xinmin Ding[21], Yang Yue[22], Huanqian Wang[22], Chi Chen[22], Jingrui Pang[1,22], YuXi Qian[23], Haoran Geng[24], Lianli Gao[2], Haiyuan Li[4], Bin Fang[4,1], Gao Huang[22,1], Yaodong Yang[11,1,25], Hao Dong[11,1], He Wang[11,13,1], Hang Zhao[22,14], Yadong Mu[11,1], Di Hu[6,1], Hao Zhao[22,1], Tiejun Huang[11,1], Shanghang Zhang[11,1‡], Yonghua Lin[1‡], Zhongyuan Wang[1‡], Guocai Yao[1†‡]

[1]Beijing Academy of Artificial Intelligence, [2]University of Electrical Science and Technology of China, [3]Ant Digital Technologies, Ant Group, [4]Beijing University of Posts and Telecommunications, [5]Harbin Institute of Technology, [6]Renmin University of China, [7]Chinese Academy of Sciences, [8]Huazhong University of Science and Technology, [9]University of Cambridge, [10]Harbin Engineering University, [11]Peking University, [12]Southwest Jiaotong University, [13]Galbot, [14]Galaxea, [15]Leju Robotics, [16]Agilex Robotics, [17]TQ-Artisan, [18]AI² Robotics, [19]Realman Robotics, [20]Booster Robotics, [21]DORA Community, [22]Tsinghua University, [23]Stanford University, [24]University of California, Berkeley, [25]PsiBot

* Equal Contribution, † Project Leaders, ‡ Corresponding Authors

shihan.wu.koorye@outlook.com, gcyao1@baai.ac.cn

https://flagopen.github.io/RoboCOIN/



Fig. 1: Overview of our **RoboCOIN** dataset. **RoboCOIN** is a large-scale, **multi-embodiment dataset explicitly built for bimanual robotic manipulation research**. It supports **15** distinct robotic platforms, with **180K+** high-quality manipulation demonstrations spanning **421** structured bimanual tasks and **16** diverse interactive scenarios. The dataset is fully open to the research community, equipped with a ready-to-use one-click installation toolchain, and can be directly deployed via the simple command *"pip install robocoin"*.

Abstract—**Despite the critical role of bimanual manipulation in endowing robots with human-like dexterity, large-scale and diverse datasets remain scarce due to the significant hardware heterogeneity across bimanual robotic platforms. To bridge this gap, we introduce RoboCOIN, a large-scale multi-embodiment bimanual manipulation dataset comprising over 180,000 demonstrations collected from 15 distinct robotic platforms. Spanning 16 diverse environments—including residential, commercial, and industrial settings—the dataset features 421 bimanual tasks systematically categorized by 39 bimanual collaboration actions and 432 objects. A key innovation of our work is the hierarchical capability pyramid, which provides granular annotations ranging from trajectory-level concepts to segment-level subtasks and frame-level kinematics. Furthermore, we present CoRobot, an efficient data processing pipeline powered by the Robot Trajectory Markup Language (RTML), designed to facilitate quality assessment, automated annotation, and unified multi-embodiment and data management. Extensive experiments demonstrate the effectiveness of RoboCOIN in enhancing the performance of various bimanual manipulation models across a wide spectrum of robotic embodiments. The entire dataset and codebase are fully open-sourced, providing a valuable resource for advancing research in bimanual and multi-embodiment manipulation.**

I. Introduction

Bimanual manipulation is pivotal for enabling robots to perform complex, human-like tasks in unstructured real-world environments, ranging from manufacturing [37] and home assistance [18] to logistics [14]. Critical to this ability is high-quality bimanual demonstration data, which underpins data-driven methods that require large-scale, diverse datasets, particularly those tailored for **multi-embodiment** scenarios, to generalize effectively across different robotic platforms [54, 9]. Such data empowers models to master complex collaboration strategies, and develop robust control policies.

Despite significant progress in data-driven robotics, existing datasets remain constrained by limited diversity and structure, particularly for bimanual tasks and multi-embodiment learning. The hardware heterogeneity across bimanual platforms impedes the collection of large-scale, diverse datasets [52]. In addition, current benchmarks primarily supply low-level action trajectories while neglecting the structural learning of the manipulation process [36]. Such limitations hinder the development of robotic platforms that can support learning systems capable of generalizing to novel environments [30, 56].

To bridge this gap, we propose **RoboCOIN**, a comprehensive **multi-embodiment bimanual manipulation** dataset comprising over 180,000 demonstrations across 421 distinct bimanual tasks, integrated with 16 diverse real-world scenarios. As depicted in Figure 1, RoboCOIN is explicitly collected from 15 diverse robotic platforms, which include three distinct bimanual configurations: bimanual robots, half-humanoid robots, and humanoid robots. These platforms are outfitted with a suite of cameras *(e.g. head, wrist, etc.)* to provide diverse perspectives for comprehensive observation. They are also equipped with both parallel grippers and dexterous hands, which encompass a variety of configurations for heterogeneous bimanual embodiments. All data are acquired via human teleoperation [11] to ensure high quality and diversity, accompanied by detailed language annotations. Besides, a two-dimensional taxonomy based on action collaboration and object flexibility structures demonstrations to enable systematic task design and progressive skill acquisition.

To enable effective structural learning across diverse embodiments, RoboCOIN introduces a **Hierarchical Capability Pyramid** with three structured annotation levels: *i) Trajectory-level* annotations capture global concepts and task objectives for holistic planning; *ii) Segment-level* annotations decompose tasks into executable subtasks with temporal alignment for structured reasoning; and *iii) Frame-level* annotations provide dense details, including kinematic states and action labels for precise control. This multi-resolution pipeline supports learning from high-level conceptual understanding to low-level control, facilitating advanced reasoning and generalization in bimanual manipulation.

Additionally, we introduce **CoRobot**, a data processing pipeline for efficient development and deployment of RoboCOIN, which integrates three key components: *i) A Robot Trajectory Markup Language (RTML)* evaluator that validates trajectory properties, to ensure physical and semantic integrity across diverse robotic platforms; *ii) A Hierarchical Annotation Pipeline* to automatically generate multi-level annotations from raw demonstration data; and *iii) A Unified Robotic Interface* which extends LeRobot [7] framework to provide unified multi-embodiment control, data management, and deployment capabilities for bimanual manipulation research. This integrated infrastructure ensures consistent data quality across diverse hardware platforms while providing the necessary tools for scalable multi-embodiment learning.

Comprehensive evaluations across diverse models and robotic platforms validate notable performance improvements for bimanual manipulation tasks. In the simulation environment, relative gains reach **75.7%** on *ARX-X5* and **212.9%** on *Franka Emika Panda* for bimanual manipulation tasks. Real-world experiments further show substantial gains from the hierarchical pyramid, with **53.6%** in-distribution and **155.6%** out-of-distribution relative improvements. Additionally, RTML filters out **35.3%** of low-quality trajectories, yielding a **22.2%** relative performance boost, demonstrating the importance of high-quality demonstration data.

The key contributions of this work are as follows:

- **A Large-scale Dataset.** We introduce RoboCOIN, a large-scale multi-embodiment bimanual dataset comprising over 180,000 demonstrations across 421 tasks, collected from 15 distinct robotic platforms, with hierarchical annotations from trajectory to frame levels.
- **An Efficient Data Processing Pipeline.** We develop a unified data processing pipeline named CoRobot, including RTML-based assessment, an automated annotation pipeline, and a platform for unified multi-embodiment dataset management and robot deployment.
- **Comprehensive Evaluations.** We perform extensive experiments across a wide spectrum of robotic platforms, demonstrating the effectiveness of RoboCOIN in enhancing bimanual manipulation models.

II. Related Work

Robotic Learning Datasets. The evolution of robot learning has been significantly driven by the availability of diverse and scalable demonstration datasets. Early robot learning, limited by hardware, relied on simulation datasets *(e.g., Meta-world [57], LIBERO [27], CALVIN [32])* but faced sim-to-real transfer challenges [60]. Open-X-Embodiment [36] aggregates real-world multi-embodiment data for better generalization but is limited to single-arm tasks, hindering its use for complex real-world bimanual interactions. The π_0 dataset [5] provides extensive long-horizon bimanual trajectories but is proprietary and closed-source, restricting access for most researchers. Recent datasets *(e.g. AgiBot World [6], Galaxea Open-World [22])* address the need for large-scale open-world bimanual data. AgiBot World offers large-scale, industrial-grade multi-scenario data, while Galaxea Open-World provides high-quality, fine-grained annotations from a unified mobile bimanual platform. However, these datasets often rely on a single robot embodiment, limiting their multi-embodiment applicability. Generally, existing datasets lack multi-embodiment bimanual data with structured hierarchical annotations, constraining the development of generalizable bimanual manipulation models.

Robotic Learning Policies. Robot learning policies have advanced from specialized small-scale models to large-scale generalist systems, particularly for bimanual manipulation. Early methods *(e.g. ACT [59], Diffusion Policy [10])* performed adequately on specific tasks with small datasets but were limited by data scale and diversity, driving the development of generalist Vision-Language-Action (VLA) models. For example, Octo [48] (trained on Open X-Embodiment dataset [36]) supports language and goal-image conditioning, enabling zero-shot adaptation to new tasks or robots. OpenVLA [25], by contrast, uses an LLM-based autoregressive architecture, tokenizing continuous actions into discrete representations for LLM compatibility. For bimanual manipulation specifically, RDT [29] stands as a pioneering diffusion-based foundation model, which learns from diverse modalities via a scalable transformer and an interpretable unified action space tailored to bimanual collaboration. π_0 [5] is a model specifically designed for bimanual manipulation, using a flow-matching architecture, combining a VLM for perception and reasoning with an action expert for high-precision continuous motor commands. GR00T-N1 [34] is dedicated to bimanual humanoid manipulation and introduced a dual-system architecture for humanoids, with GR00T-N1.5 [35] adding upgrades like an improved VLM and FLARE objective. Specialized models *(e.g. Agibot GO-1 [6], Galaxea G0 [22], RoboBrain-X0 [47, 21])* enable effective single-embodiment bimanual control via multi-stage training and hierarchical systems. All these models have their respective advantages, while the models designed for precise bimanual control rely on high-quality and diverse bimanual manipulation data. Despite their scale, these bimanual-related models lack structured task hierarchy understanding, limiting their reasoning ability for complex bimanual tasks.

III. RoboCOIN Dataset

RoboCOIN is introduced as a pioneering **multi-embodiment bimanual manipulation** dataset, featuring a comprehensive suite of hierarchical annotations designed to facilitate advanced robot learning. It integrates 15 diverse robotic platforms, 180K+ high-quality demonstrations, 421 structured bimanual tasks, and 16 real-world scenarios. A Hierarchical Capability Pyramid is introduced to span three levels of annotations, facilitating multi-resolution learning from high-level concepts to low-level control.

A. Data Collection and Storage

We use a diverse set of 15 robotic platforms for comprehensive data acquisition, encompassing bimanual, half-humanoid, and humanoid configurations to ensure broad applicability across different bimanual manipulation scenarios. Figure 2 illustrates three representative platforms: bimanual robots *(e.g., AgileX Cobot Magic [41])*, half-humanoid robots *(e.g., Realman RMC-AIDA-L [44])*, and humanoid robots *(e.g., Unitree G1edu-u3 [50])*. We employs teleoperation to ensure high-quality data collection, utilizing methods such as leader-follower isomorphic arms, exoskeletons, and motion capture systems, etc. The platforms are equipped with a comprehensive suite of cameras, including head-mounted and wrist-mounted (chest, back, and third-person cameras for some platforms) to provide multi-view visual observations. Featuring both parallel grippers and dexterous hands, kinematic data is recorded at high frequency to capture joint angles, end-effector poses, and gripper states, supporting accurate monitoring of robot motion, object interactions, and the diverse configuration characteristics of different platforms. All kinematic measurements adhere to standardized conventions to ensure consistency across diverse robotic platforms, with joint states measured in radians and gripper states normalized between 0 and 1. The end-effector state includes position and orientation, where distances are expressed in meters, orientation is represented using Euler angles in radians, and all parameters follow a unified right-handed coordinate system with x-forward, y-left, and z-up. Strict temporal synchronization across all data streams is maintained through timestamp alignment, ensuring consistency between visual observations and kinematic states. Table I provides a detailed overview of the robotic platforms used in RoboCOIN, including their arm degrees of freedom (DoF), camera configurations, gripper types, and teleoperation methods. This diverse set of platforms ensures that the collected data covers a wide range of bimanual operational scenarios, from basic dual-arm control to complex humanoid bimanual interaction, laying a solid foundation for cross-embodiment bimanual learning.

B. Statistics and Taxonomy

Robotic Platforms. RoboCOIN is explicitly designed as a multi-embodiment foundation to ensure broad applicability across diverse robotic platforms. Figure 3(a) shows the distribution of robotic platforms in RoboCOIN, encompassing dual-arm, half-humanoid, and humanoid types. The 15 distinct plat-

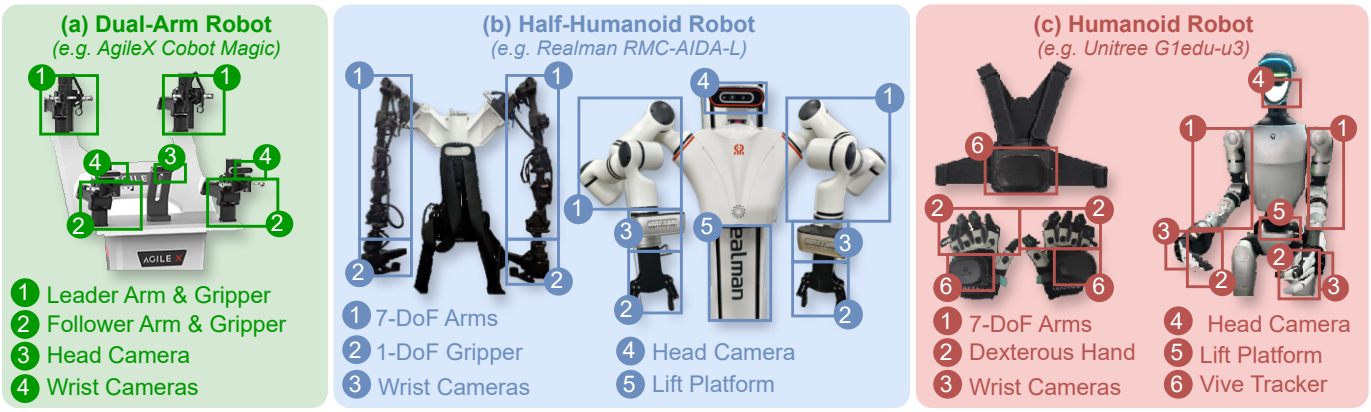


Fig. 2: **Data collection platforms of our RoboCOIN**. *(a) Dual Robot (e.g., AgileX Cobot Magic).* A bimanual robot with two 6-DoF arms and parallel grippers, capable of performing complex bimanual tasks. *(b) Half-Humanoid Robot (e.g., Realman RMC-AIDA-L).* Left: wearable teleoperation device for human demonstration, right: bimanual robot with parallel grippers. *(c) Humanoid Robot (e.g., Unitree G1edu-u3). Left:* Wearable motion capture device for human demonstration. *Right:* Humanoid robot with advanced dexterous manipulation capabilities. Head and wrist cameras provide multi-view visual observations.

TABLE I: Robotic platforms used in RoboCOIN dataset collection.

Type	Name	Arm DoF	Camera Configuration	Gripper Type	Teleoperation Method
Dual-Arm	Agilex Cobot Magic [41]	2×6	Head + Wrist	Parallel Gripper	Isomorphic Arm
	Agilex Split ALOHA [41]	2×6	Head + Wrist	Parallel Gripper	Isomorphic Arm
	Galaxea R1 Lite [16]	2×6	Head + Wrist	Parallel Gripper	Isomorphic Arm
Half-Humanoid	Realman RMC-AIDA-L [44]	2×7	Head + Wrist	Parallel Gripper	Exoskeleton
	Agibot G1 [1]	2×7	Head + Wrist + Back	Parallel Gripper	Virtual Reality
	AI^2 AlphaBot 2 [42]	2×7	Head + Wrist + Chest	Dexterous Hand	Virtual Reality / Isomorphic Arm
	AI^2 AlphaBot 1s [42]	2×7	Head + Wrist + Chest	Dexterous Hand	Virtual Reality / Isomorphic Arm
	Galbot G1 [17]	2×7	Head + Wrist	Parallel Gripper	Motion Capture
	Tianqing A2 [49]	2×7	Head + Wrist + Back	Parallel Gripper	Virtual Reality
	Realman Rs-02 [44]	2×7	Head + Wrist	Parallel Gripper	Exoskeleton
	Realman Rs-01 [44]	2×7	Head + Wrist	Parallel Gripper	Exoskeleton
	Airbot MMK2 [2]	2×6	Head + Wrist + Third-Person	Dexterous Hand	Virtual Reality
	Leju Kuavo 4 LB [43]	2×7	Head + Wrist	Dexterous Hand	Virtual Reality
Humanoid	Leju Kuavo 4 Pro [43]	2×7	Head + Wrist	Dexterous Hand	Virtual Reality
	Unitree G1edu-u3 [50]	2×7	Head + Wrist	Dexterous Hand	Motion Capture / Exoskeleton

forms offer rich morphological diversity for complex bimanual manipulation, with each type featuring unique characteristics tailored to different bimanual manipulation scenarios:

- **Dual-arm Robots (33.2%).** Comprising 3 distinct models, these platforms focus on core dual-arm manipulation capabilities, making them suitable for fundamental bimanual tasks while maintaining low hardware costs.
- **Half-humanoid Robots (49.0%).** As the mainstream architecture in RoboCOIN, this category includes 10 distinct platforms. Among them, 45% are equipped with standard parallel grippers, while 4% feature dexterous hands, balancing human-like movement patterns with practical hardware requirements.
- **Humanoid Robots (17.8%).** Consisting of 2 platforms, these robots are equipped with fully dexterous hands, delivering advanced human-like manipulation capabilities.

This multi-embodiment platform portfolio ensures support for a wide spectrum of bimanual tasks, ranging from basic collaboration to complex dexterous manipulation.

Scenarios. As shown in Figure 3(b), data collection spans 16 distinct scenarios, categorized into three main environments to ensure broad applicability:

- **Residential Scenarios (47.1%).** As the primary scenario, it covers daily bimanual tasks such as cooking, cleaning, and home organization, which are closely aligned with human daily life scenarios.
- **Commercial Scenarios (18.6%).** Including restaurant, courier, supermarket, and amusement scenarios, it focuses on bimanual collaboration tasks *(e.g., order picking, goods handling)* that require frequent interaction between both hands.
- **Working Scenarios (34.3%).** Covering factory, office, laboratory, and other scenarios, it supports complex bimanual operations such as equipment debugging and material handling.

Each category includes finer-grained scenarios *(e.g., commercial settings cover restaurants, courier services, supermarkets, etc.)*, covering diverse real-world applications.

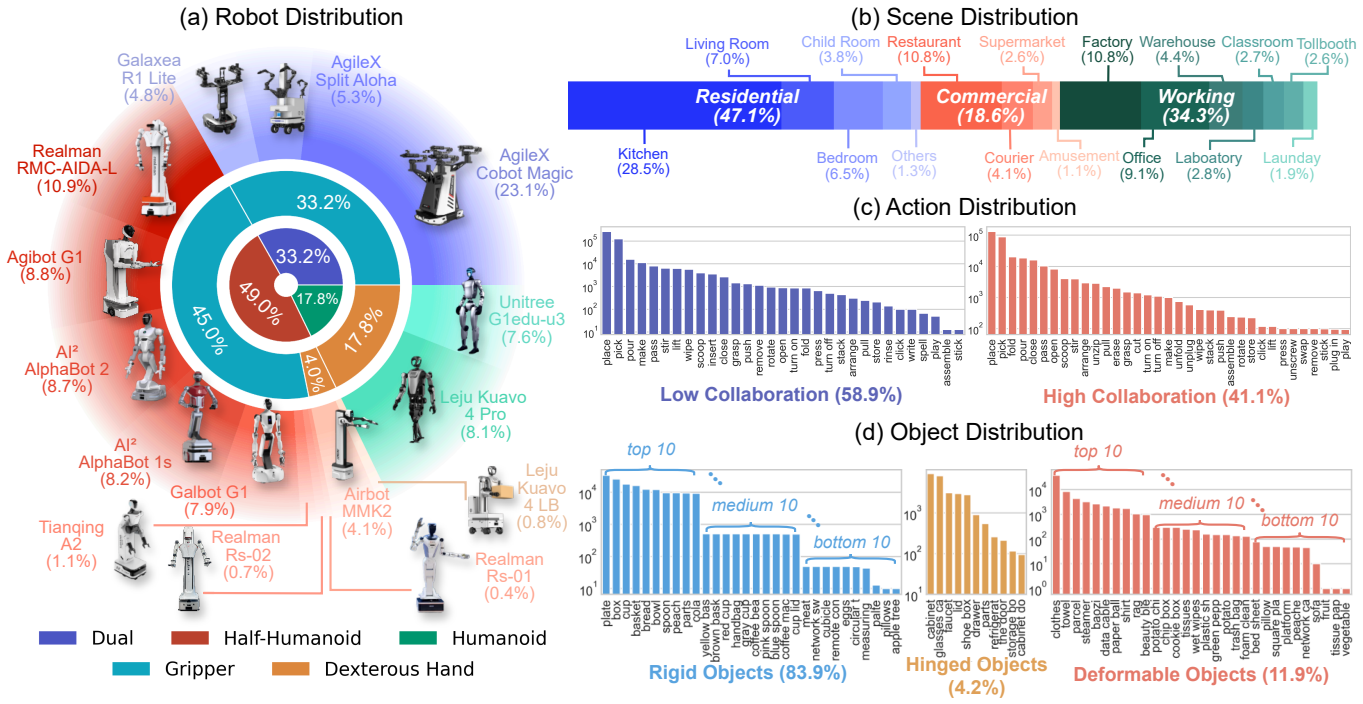


Fig. 3: **Overview statistics of the RoboCOIN dataset.** RoboCOIN incorporates (a) 15 distinct robotic platforms, including bimanual, half-humanoid, and humanoid robots with grippers and dexterous hands; (b) 16 diverse environments such as residential, commercial, and working scenes; (c) 39 action types categorized by collaboration levels; and (d) 432 object types spanning rigid, articulated, and deformable categories.

Task Taxonomy. RoboCOIN employs a two-dimensional task taxonomy that organizes manipulation scenarios along action collaboration (Figure 3(c)) and object flexibility (Figure 3(d)). Specifically, 39 action patterns are categorized by the degree of bimanual collaboration required, including:

- **Low-collaboration Tasks (58.9%).** Tasks where the two arms operate largely sequentially, with minimal synchronous interaction between the two arms.
- **High-collaboration Tasks (41.1%).** Tasks featuring partial or fully parallel arm movements, requiring close synchronous cooperation between the two arms.

To ensure the uniqueness of each action's meaning and avoid terminology ambiguity, we strictly guarantee the uniqueness of each action's definition, and a synonym mapping mechanism has been designed to standardize terminology usage. The details can be founed in **Appendix A**.

Similarly, 432 objects are classified along a spectrum of mobility, which can be divided into three types:

- **Rigid Objects (83.9%).** Objects with fixed poses that do not undergo shape changes.
- **Hinged Objects (4.2%).** Objects with articulated parts that can move relative to each other.
- **Deformable Objects (11.9%).** Objects that can undergo significant shape changes across most parts.

This integrated framework facilitates the creation of diverse and incrementally challenging tasks that support skill development across different robotic platforms and real-world settings.

C. Hierarchical Capability Pyramid

As illustrated in Figure 4, the hierarchical capability pyramid in RoboCOIN encompasses three levels of structured annotations: *trajectory-level, segment-level, and frame-level*, enabling multi-resolution learning from high-level conceptual understanding to low-level control.

Trajectory-level Concepts. Trajectory-level annotations capture task concepts by characterizing the overall scene configuration. This involves a description of the scene, detailing the environment settings and the placement of objects. The resulting unified representation enables global spatial and physical reasoning throughout the entire task sequence [58, 45].

Segment-level Subtasks. Segment-level annotations decompose tasks into specific subtasks, which may temporally overlap to accommodate dual-arm operations. Each segment is aligned with specific video frames and includes step-by-step instructions. Annotations also explicitly label exception cases, such as grasping failures, to support robust error handling. This structured decomposition facilitates learning of temporal reasoning and task planning [3, 46].

Frame-level Kinematics. Frame-level annotations describe kinematics for each frame. This includes the motion parameters *(e.g., direction, velocity, acceleration)* for both arm end-effectors, and the status of grippers or dexterous hands *(such as open/close state or transitioning movements)*. This high-density kinematic data enables real-time intrinsic feedback control and precise motion execution [55].

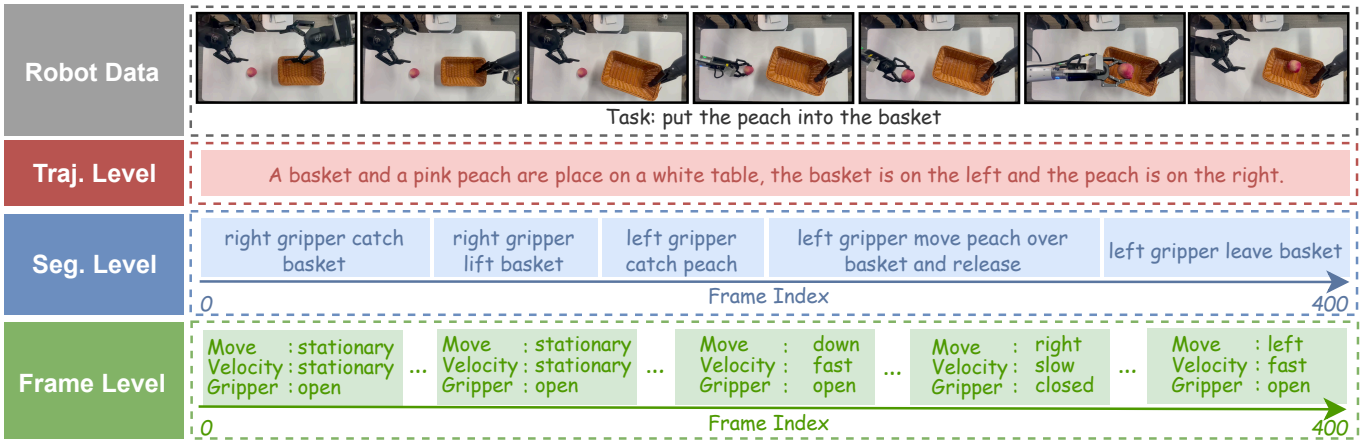


Fig. 4: **Hierarchical capability pyramid of RoboCOIN**. **Trajectory-level Annotations** define the global concepts; **Segment-level Annotations** decompose the task into executable subtasks; and **Frame-level Annotations** provide dense low-level details such as motion trajectories and gripper states. All annotations are temporally synchronized to form a cohesive data structure.

TABLE II: **Qualitative comparison of existing real-world datasets for robot manipulation.** All data is drawn from the original paper or the RoboMIND paper. N/A indicates that the dataset does not provide explicit annotations for the corresponding attribute. † Not a dataset in itself, but an aggregation of existing datasets.

Dataset	Arm	Embodiments	Trajectories	Tasks	Actions	Dexterous	Annotation	Collection Method
Pinto and Gupta [38]	Dual	1	50k	N/A	1	✗	No	Scripted
RoboNet [12]	Single	1	162k	N/A	N/A	✗	No	Scripted
MT-Opt [23]	Single	1	800k	12	1	✗	No	Scripted
BridgeData [13]	Single	1	7.2k	71	4	✗	No	Human Teleoperation
BC-Z [20]	Single	1	26k	100	3	✗	No	Human Teleoperation
RH20T [15]	Single	1	13k	140	33	✗	No	Human Teleoperation
RoboSet [4]	Single	1	98k	38	6	✗	No	30% Human / 70% Scripted
BridgeData V2 [51]	Single	1	60k	N/A	13	✗	No	85% Human / 15% Scripted
DROID [24]	Single	1	76k	N/A	86	✗	No	Human Teleoperation
Open X-Embodiment† [36]	Single+Dual	22	1.4M	160k	217	✗	No	Dataset Aggregation
RoboMIND [53]	Single+Dual	4	107k	479	38	✓	Flat	Human Teleoperation
AgiBot World Beta [6]	Dual	1	1M	217	87	✗	Flat	Human Teleoperation
Open Galaxea [22]	Dual	1	50k	150	58	✓	Flat	Human Teleoperation
RoboCOIN (Ours)	**Dual**	**15**	180K+	421	39	✓	**Hierarchical**	Human Teleoperation

D. Comparison with Existing Datasets

As shown in Table II, RoboCOIN distinguishes itself from existing robot datasets with its open, generalizable design for complex bimanual manipulation. Most existing datasets are limited to single-arm robots *(e.g., BridgeData V2 [51], DROID [24])*, mixed-embodiment datasets with insufficient bimanual coverage *(e.g., Open X-Embodiment [36], RoboMIND [53])*, or single-platform dual-arm datasets *(e.g., AgiBot World Beta [6], Open Galaxea [22])*. In contrast, RoboCOIN includes 15 diverse platforms with parallel grippers and dexterous hands, plus a hierarchical capability pyramid with multi-level annotations. As a unique, fully open-source dataset, it provides comprehensive multi-embodiment bimanual manipulation data, serving as an invaluable resource for advancing multi-embodiment bimanual manipulation research.

IV. CoRobot Data Processing Pipeline

For the efficient construction of the RoboCOIN dataset, we developed a CoRobot, an integrated data processing pipeline, as illustrated in Figure 5. This pipeline encompasses three key components: *i)* the Robot Trajectory Markup Language (RTML) for automated trajectory validation, *ii)* a hierarchical annotation pipeline for generating rich and structured task descriptions, and *iii)* a unified robotic interface for standardized robot control and multi-embodiment data management.

A. Robot Trajectory Markup Language Evaluation

High-quality data collection is challenged by distribution shifts arising from human operators' varying expertise, which deleteriously impact model performance. To address this problem at the source, we propose the Robot Trajectory Markup Language (RTML), a domain-specific language designed to convert expert rules into standardized, machine-readable, and configurable constraints (Figure 5 (a)). The design of RTML is based on three key principles for high-quality robot motion:

- **Motion Stability.** Trajectories should be smooth and predictable, avoiding sudden changes that could lead to instability or inaccuracies.
- **Pose Consistency.** During the task execution phase, the robot's end-effector pose must meet task-specific con-

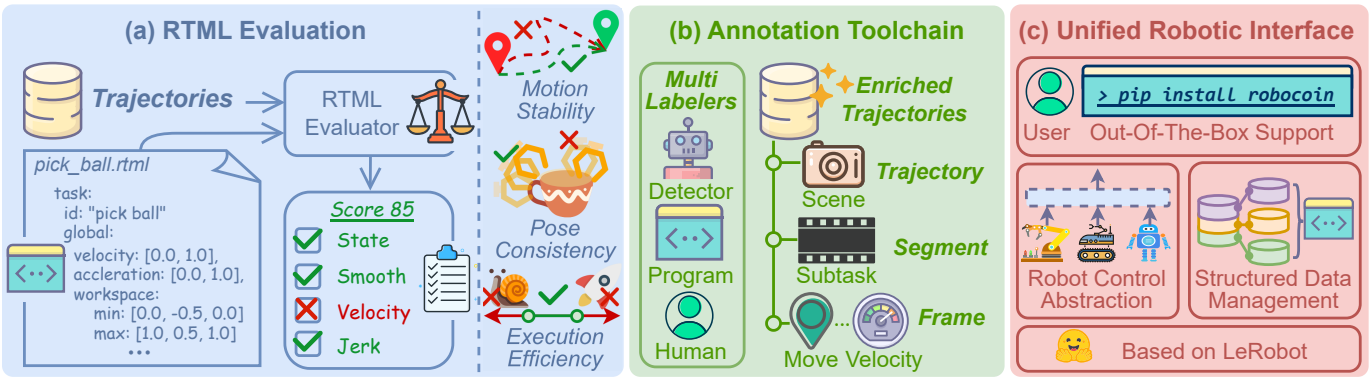


Fig. 5: **Overview of the CoRobot data processing pipeline.** (a) Robot Trajectory Markup Language (RTML) for automated trajectory validation. (b) Annotation Pipeline for generating rich and hierarchical task descriptions. (c) An out-of-the-box Unified Robotic Interface for unified robot control and multi-embodiment data management.

straints to ensure successful execution.

- **Execution Efficiency.** A trajectory must balance speed and precision, avoiding excessive haste or hesitation.

RTML is defined using the YAML format for readability and ease of use. It constrains trajectories from two perspectives: *i)* global constraints that apply to the entire trajectory, defining motion characteristics including workspace boundaries, velocity limits, acceleration limits, and duration limits; and *ii)* local constraints that divide the trajectory into sequential phases *(e.g., approach, grasp and place)*, defining override parameters and orientation tolerances for each phase. Furthermore, an RTML evaluator is provided to automatically assess trajectory quality against the defined constraints. The output includes detailed reports and an overall quality score, providing quantitative support for data selection and filtering. The detailed specification of RTML can be found in **Appendix B**.

B. Annotation Pipeline

We present a hierarchical annotation pipeline integrating detectors, rule-based programs, and human refinement, comprising three pipelines (Figure 5 (b)):

- **Trajectory-Level.** We use open-vocabulary detectors [28, 40] to localize objects and their spatial coordinates, which are fed into Large Language Models [26] to generate high-level scene descriptions, establishing semantic context for action understanding.
- **Segment-Level.** Rule-based tools identify potential segmentation points *(e.g., gripper opening/closing)* under human-specified guidance, with human annotators fine-tuning these points and filling in annotations.
- **Frame-Level.** A cascaded sliding window framework extracts gripper kinematics. Taking displacement calculation as an example: the gripper's displacement at frame t (denoted as m_t) is calculated by subtracting the 3D coordinates of the gripper at the n-th preceding frame (x_{t-n}) from its coordinates at the current frame (x_t), i.e., $m_t = x_t - x_{t-n} = (x_t^x - x_{t-n}^x, x_t^y - x_{t-n}^y, x_t^z - x_{t-n}^z)$. For other kinematic indicators *(e.g., velocity, acceleration)*, the sliding window calculation uses the previous window's output as input, enabling the extraction of higher-order motion features. Finally, predefined thresholds convert these numerical kinematic metrics into consistent text labels, enabling fine-grained kinematic annotation.

After the automatic annotation process, human annotators review and refine the annotations to ensure accuracy. Detailed implementations and analysis are provided in **Appendix C**.

C. Unified Robotic Interface

The heterogeneity of robot hardware interfaces, control protocols, and data representations presents a critical barrier to scalable multi-embodiment learning. To alleviate these challenges, we introduce a Unified Robotic Interface that consolidates robot control and data management within a unified infrastructure (Figure 5(c)). Built on the LeRobot framework [7], the interface forms a robust, modular software stack with the following core functionalities:

- **Unified Control Abstraction.** The interface integrates vendor-provided robot SDKs and is compatible with both ROS and ROS 2[39, 31], delivering a homogeneous control layer across diverse hardware. It unifies device management and control paradigms, like camera configuration, coordinate alignment, and joint unit normalization, enabling consistent cross-embodiment operation.
- **Structured Data Management.** To enable efficient dataset reuse and flexible training data composition, the interface adopts an atomic data storage strategy that partitions datasets into minimal, reusable subsets tagged by embodiment, task type, and environment. This structured approach allows researchers to easily query and assemble training data tailored to specific research needs.

By enabling one-click deployment through "pip install robocoin", the proposed interface effectively reduces engineering barriers for multi-embodiment learning research. The system is fully open-source to support reproducibility and community-driven extensions. [1]

[1]https://github.com/FlagOpen/CoRobot

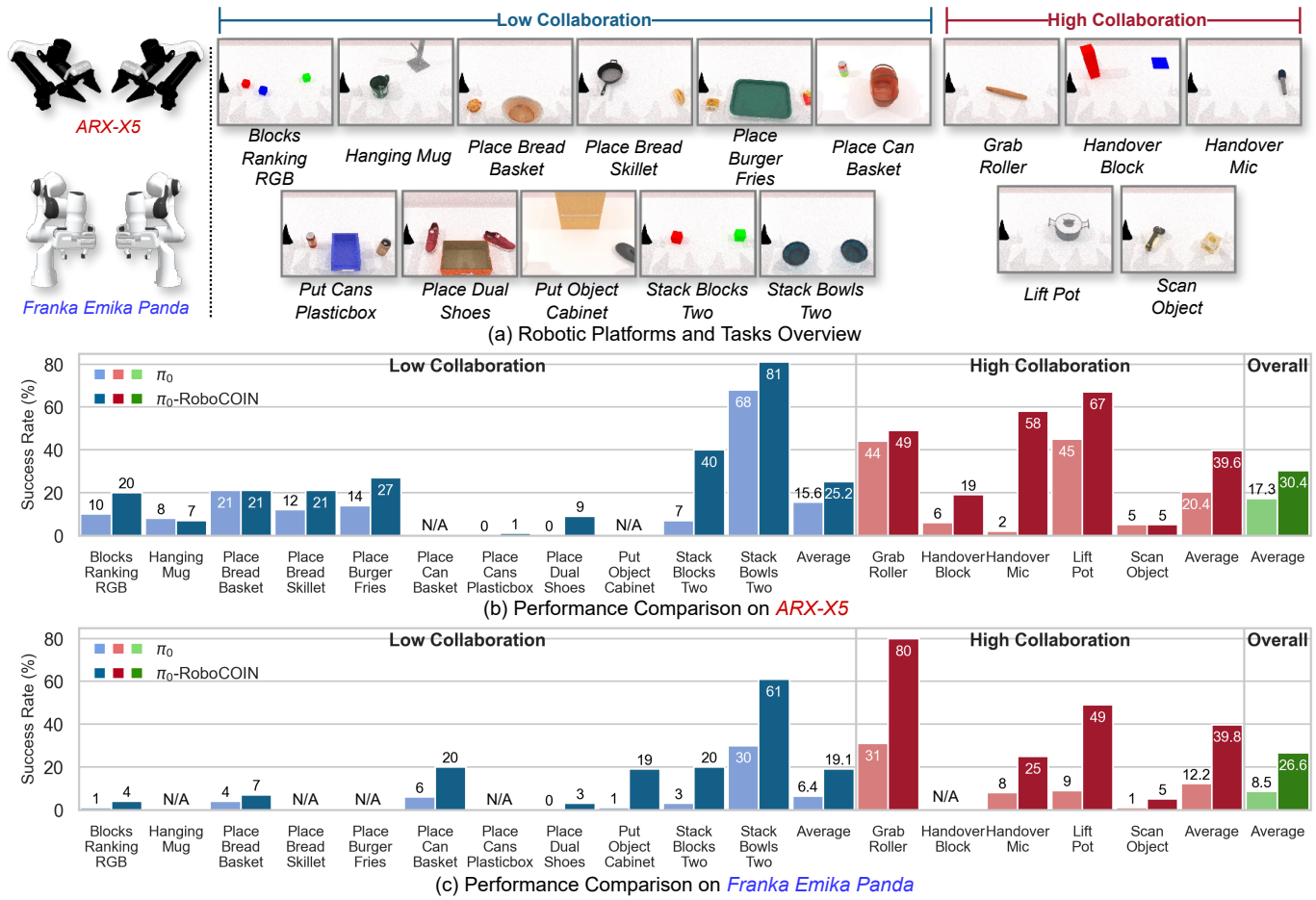


Fig. 6: **Cross-embodiment transfer results on RoboTwin 2.0.** (a) Our selected robotic platforms and bimanual tasks in the *RoboTwin 2.0* environment. (b) Performance comparison on *ARX-X5*. (c) Performance comparison on *Franka Emika Panda*. N/A indicates that the trajectory generation failed on this task.

V. Experiments and Analysis

In this section, we evaluate the effectiveness of the RoboCOIN dataset through comprehensive experiments in both simulation and real-world environments. We aim to answer the following research questions:

> ***Q1.*** *How does the RoboCOIN dataset enhance the multi-embodiment capability of VLA models?*
> ***Q2.*** *Does the hierarchical capability pyramid improve VLA models, and in what aspects?*
> ***Q3.*** *To what extent does the RTML contribute to improving data quality and model performance?*

A. Experiment Setup

Simulation Environment. The simulation experiment focuses on ***Q1***. We conduct evaluations in the *RoboTwin 2.0* environment [33, 8] using two distinct dual-arm platforms: *ARX-X5* and *Franka Emika Panda*, both of which are unseen embodiments in the training dataset. We design 16 dual-arm manipulation tasks of varying difficulty, and as trajectory generation failed on a subset of tasks, we evaluate *ARX-X5* on 14 tasks and *Franka Emika Panda* on 11 tasks, respectively. Visual observations are captured by *Realsense D435* cameras mounted on the head and wrists, with a resolution of 320×240.

Real-World Environment. The real experiments focus on ***Q2*** and ***Q3***, using two robotic platforms: the *Realman RMC-AIDA-L* [44] and the *Unitree G1edu-u3* [50]. The *Realman RMC-AIDA-L* is equipped with three *Realsense D435 Cameras* and *RMG24 Parallel Grippers* for visual perception and manipulation. On this platform, tasks are designed with varying complexity according to the difficulty of dual-arm collaboration and object flexibility, also covering out-of-distribution (OOD) test scenarios. The *Unitree G1edu-u3* is integrated with a *Realsense D435 Camera* on the head and *Realsense D405 Cameras* on the wrists, along with the *Unitree Dex3-1 Three-fingered Dexterous Hand*. For this platform, two representative tasks are adopted to investigate how trajectory data quality affects policy learning.

Representative Tasks. To better illustrate task execution pipelines and inherent challenges, we select several representative tasks from our experiments for detailed description, including both simulated and real-world settings:

- **Simulation Lift Pot.** The robot grasps both handles of a pot with two arms and lifts it off the ground. The task succeeds when the pot is fully separated from the ground. The main challenge is highly synchronous bimanual collaboration to prevent tilting or dropping.
- **Simulation Place Dual Shoes.** The robot grasps two shoes at the same time and places them into a box one after another. The task succeeds when both shoes are completely inside the box. This task demands bimanual collaboration and accurate placement control.
- **Real-World Peach Drawer.** The robot uses one arm to place a peach into a drawer and the other to close the drawer. The task succeeds when the peach is inside the drawer and the drawer is fully closed. It requires precise asynchronous action execution.
- **Real-World Pass Bowl.** The robot hands a bowl from one arm to another in mid-air and places it at the target position. The task succeeds when the bowl is stably placed at the target. The key difficulty lies in stable handover and tight bimanual collaboration.

The detailed simulation and real-world experimental settings and visual sequences can be found in **Appendix D**.

Evaluated VLA Policies. To comprehensively validate the generalization capability of our proposed framework across diverse robotic platforms, we evaluate two state-of-the-art VLAs specifically designed for bimanual manipulation tasks:

- π_0 [5]. A flow-matching-based VLA model with a large vision-language model and a action expert network.
- **GR00T N1.5** [35]. A dual-system VLA model for humanoid robots, featuring a vision-language model and a future state alignment objective.

To enable parameter-efficient adaptation, we fine-tuned both models on data from all experimental tasks (with 50 trajectories per task) in a joint training manner: π_0 using LoRA [19], while *GR00T N1.5* was adapted via partial fine-tuning on only its diffusion and projector components. For π_0, we used the AdamW optimizer with a learning rate of 2.5×10^{-5}, batch size 32, 30000 training steps. For *GR00T N1.5*, we also employed AdamW optimizer, with a learning rate of 1×10^{-4}, batch size 24, 10000 training steps.

B. Impact of Multi-Embodiment Adaptability

To answer ***Q1***, we design a cross-embodiment transfer experiment based on the simulation *RoboTwin 2.0* environment with the dual-arm *ARX-X5* and *Franka Emika Panda* robots as the target embodiments. It compares the fine-tuning performance of the original model and the model post-trained on the RoboCOIN dataset.

- π_0: The baseline model fine-tuned from the original π_0 using selected *RoboTwin 2.0* tasks.
- π_0**-RoboCOIN**: The optimized model post-trained on the random sample RoboCOIN-10K subset, then fine-tuned on selected *RoboTwin 2.0* tasks.

As illustrated in Figure 6, π_0**-RoboCOIN** achieves consistent and substantial performance gains over π_0 across nearly all tasks on both robotic platforms. On the *ARX-X5* platform, π_0**-RoboCOIN** improves the average success rate from **17.3%** to **30.4%**, representing a relative improvement of **75.7%**. On the *Franka Emika Panda* platform, the average success rate rises from **8.5%** to **26.6%**, delivering a **212.9%** relative improvement. Notably, high-collaboration tasks benefit significantly more from RoboCOIN than low-collaboration tasks. On *ARX-X5*, low-collaboration tasks improve moderately from **15.6%** to **25.2%** *(a relative gain of 61.5%)*, whereas high-collaboration tasks surge from **20.4%** to **39.6%**, with a remarkable relative improvement of **94.1%**. On *Franka Emika Panda*, the performance boost is even more prominent across both collaboration levels. Notably, for challenging tasks such as *"Place Dual Shoes"*, the success rate increases from **0%** to **9%** on *ARX-X5* and from **0%** to **3%** on *Franka Emika Panda*, turning previously unachievable tasks into feasible ones. This observation underscores that multi-embodiment data in RoboCOIN endows the policy with strong, transferable high-collaboration manipulation priors and effectively enhances the generalization of robotic policies to unseen hardware platforms, especially for complex high-collaboration bimanual manipulation tasks.

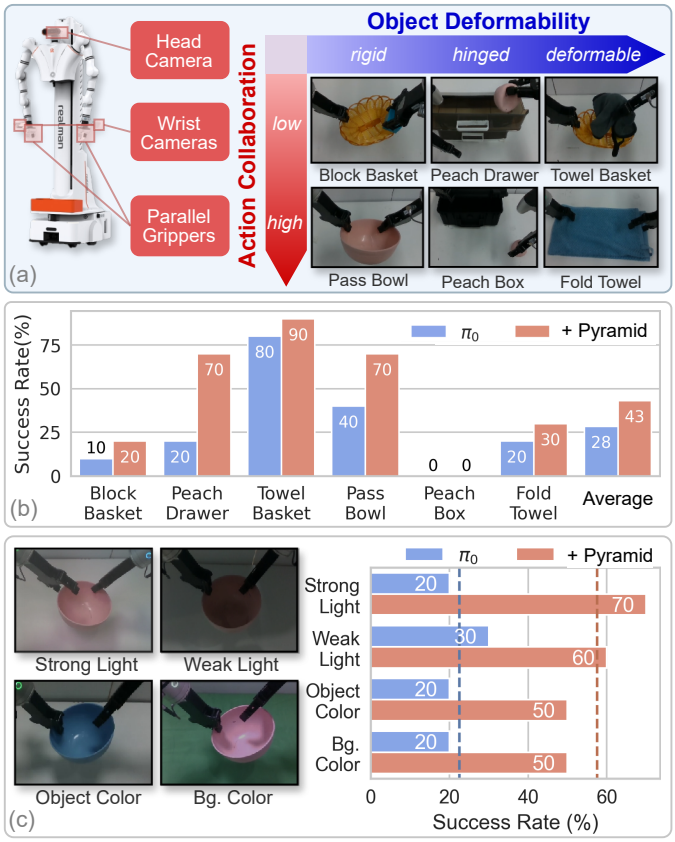


Fig. 7: **Results of Realman RMC-AIDA-L over the π_0 baseline**. It follows an multi-dimensional task design (a), with the in-distribution (b) and out-of-distribution results (c) showing the success rates with and without HAI.

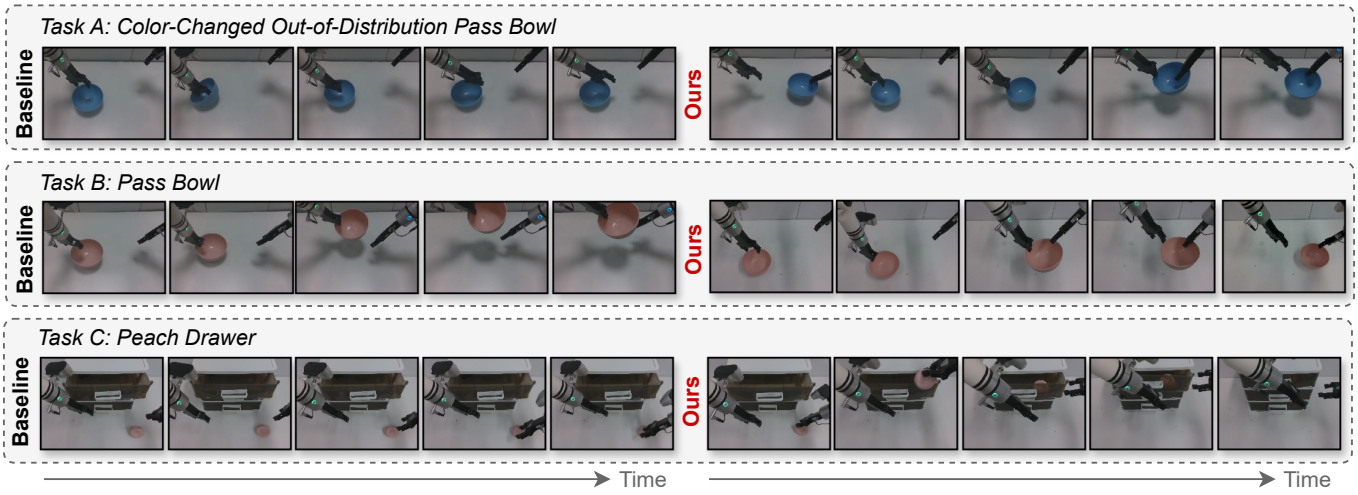


Fig. 8: **Case study** of the impact of RTML on data quality and model performance.

C. Impact of Hierarchical Capability Pyramid

To address ***Q2***, we investigate how the hierarchical capability pyramid contributes to robotic manipulation, with experiments conducted on the *Realman RMC-AIDA-L* platform using the π_0. We design two structurally consistent pipelines for controlled comparison:

- π_0 **Baseline.** The model takes raw visual observations, proprioceptive states, and standard natural language instructions as input, and directly outputs manipulation actions in an end-to-end manner.
- π_0 **+ Pyramid.** A minimal, non-intrusive integration strategy that introduces the hierarchical capability pyramid without modifying the model architecture or parameters. Specifically, we enrich the language input with structured hierarchical task, subtask, and action descriptions, which are formed by fusing human instructions and automatically extracted motion cues from trajectory history.

This design ensures the augmented model can naturally incorporate structured task priors and motion knowledge from the hierarchical capability pyramid into its decision-making process, while maintaining strict consistency with the baseline pipeline for fair comparison. Detailed implementation details of the integration strategy are provided in **Appendix E**.

In-Distribution Performance. Figure 7 (a) shows our multi-level task suite, with complexity determined by dual-arm collaboration difficulty and object flexibility. As observed in Figure 7 (b), introducing the hierarchical capability pyramid leads to consistent and significant performance gains across all tasks, with an average success rate improvement from **28%** to **43%**, representing a **53.6%** relative improvement. Notably, the success rate of the complex task *"Peach Drawer"* rises sharply from **20%** to **70%**, highlighting that the hierarchical structure is beneficial for long-horizon, highly coordinated tasks.

Out-of-Distribution Robustness. We further evaluate model robustness by directly deploying in-distribution models to four OOD variants of the *"Pass Bowl"* task, involving changes in lighting, background, and object appearance. As shown in Figure 7 (c), the benefit of the hierarchical capability pyramid remains strong under distribution shift.The average success rate across OOD tasks improves from **22.5%** to **57.5%**, representing a **155.6%** relative improvement. Compared to in-distribution results *(40% and 70%)*, the baseline π_0 suffers a **43.8%** relative performance drop, whereas the pyramid-augmented model only drops by **17.9%**. These results confirm that the hierarchical capability pyramid effectively improves robustness to environmental variations.

Qualitative Case Study. To further illustrate the functional improvements brought by the hierarchical capability pyramid at different levels, we present three representative qualitative cases covering global scene understanding, subtask transition, and fine-grained manipulation, as shown in Figure 8:

- **Color-changed Out-of-Distribution Pass Bowl (20%→50%).** The baseline fails to grasp the bowl under appearance distribution shift, while our approach completes grasping and task execution, demonstrating improved *scene-level perception and generalization*.
- **Pass Bowl (40%→70%).** The baseline gets stuck during arm handover, while our method achieves smooth subtask switching, showing enhanced *segment-level transition capability*.
- **Peach Drawer (20%→70%).** The baseline fails in fine-grained peach grasping, while our method performs stable manipulation, indicating improved *frame-level fine manipulation ability*.

Together, these cases demonstrate that the hierarchical capability pyramid systematically enhances performance across scene-level perception, segment-level subtask transition, and frame-level fine-grained manipulation—directly aligning with its multi-level structural design and validating that the pyramid's hierarchical priors effectively address the key limitations of the baseline model at each corresponding level.

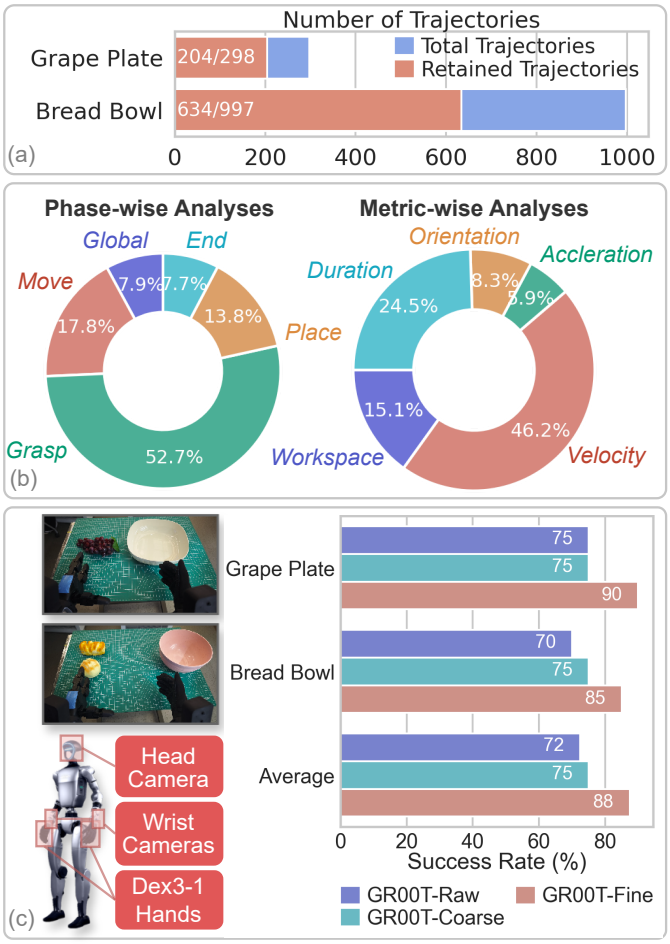


Fig. 9: **Impact of RTML on data quality and model performance.** (a) RTML filtering effect on two tasks. (b) Failure cause analysis from phase-wise and metric-wise perspectives. (c) Model performance improvement of *Unitree G1edu-u3 + GR00T N1.5* under 3 fine-tuning settings.

D. Impact of RTML

To answer ***Q3***, we conduct experiments on two tasks using the *Unitree G1edu-u3* platform. As shown in Figure 9(a), RTML filters out an average of **35.3%** of low-quality trajectories across the two tasks, indicating that the original human demonstration data contains a large amount of inconsistent information that may interfere with effective model learning, verifying the necessity of data quality optimization. Combined with phase-wise and metric-wise analyses (Figure 9(b)), the key findings are summarized as follows:

- **Phase-level analysis.** The grasping phase accounts for the highest proportion of failures (**52.7%**), followed by the moving phase (**17.8%**).
- **Metric-level analysis.** Velocity violation is the dominant cause of trajectory invalidity (**46.2%**), with duration violation as the secondary factor (**24.5%**).

Together, these observations identify critical failure modes and provide clear, actionable guidance for future demonstration collection and policy optimization.

To further investigate the impact of RTML on model performance, we further evaluated how RTML-filtered data affects policy learning by comparing three fine-tuning settings:

- **GR00T-Raw.** Fine-tuned on the original dataset without RTML filtering.
- **GR00T-Coarse.** Fine-tuned on data filtered only by global RTML constraints.
- **GR00T-Fine.** Fine-tuned on data filtered by both global and phase-wise constraints.

From the results in Figure 9(c), the three configurations exhibit a clear progressive improvement in average success rates. Compared to *GR00T-Raw* with a success rate of **72%**, *GR00T-Coarse* achieves a modest **3%** gain *(4.2% relative)*, while *GR00T-Fine* achieves a significant **16%** improvement *(22.2% relative)*. This observation highlights the important impact of phase-level constraints on trajectory quality and policy learning. These results demonstrate that RTML effectively enhances data quality by filtering out low-quality trajectories, and that this improvement in data quality translates into significant performance gains for the trained policies, especially when fine-grained, phase-specific constraints are applied.

VI. Conclusion, Limitations and Future Work

In this work, we present **RoboCOIN**, a **large-scale multi-embodiment bimanual** dataset that unifies **15 robotic platforms**, over **180,000 demonstrations**, **421 tasks**, and **16 scenarios** into a single benchmark. RoboCOIN bridges critical gaps in bimanual manipulation research by offering unprecedented hardware diversity and a hierarchical capability pyramid for structured learning. Complementing the dataset, we introduce **CoRobot**, an integrated pipeline powered by RTML for trajectory quality assessment, a semi-automatic annotation pipeline, and a unified platform for control and data management. Extensive experiments show that RoboCOIN significantly enhances multi-embodiment adaptability, hierarchical reasoning, and data quality for robotic learning, providing a solid foundation for future research in multi-embodiment bimanual manipulation.

While RoboCOIN serves as a significant catalyst for bimanual manipulation research, it is subject to several limitations that warrant further investigation. *First,* reliance on teleoperation may introduce inherent operator biases, leading to inter-operator variability in trajectory patterns. *Second,* manual annotation presents a scalability bottleneck due to its high labor costs and potential for subjectivity, which may impact data consistency. *Third,* the current RTML framework depends heavily on expert-defined heuristics, potentially constraining its flexibility when applied to niche tasks or novel robotic platforms. These limitations may affect the overall robustness and generalization of the dataset and trained models, highlighting our commitment to ongoing research efforts aimed at enhancing data quality, annotation efficiency, and RTML adaptability in future iterations of RoboCOIN.

References

[1] Agibot. https://www.agibot.com/products/G1.

[2] Airbot. https://airbots.online/mmk2.

[3] Suneel Belkhale, Tianli Ding, Ted Xiao, Pierre Sermanet, Quon Vuong, Jonathan Tompson, Yevgen Chebotar, Debidatta Dwibedi, and Dorsa Sadigh. Rt-h: Action hierarchies using language. *arXiv preprint arXiv:2403.01823*, 2024.

[4] Homanga Bharadhwaj, Jay Vakil, Mohit Sharma, Abhinav Gupta, Shubham Tulsiani, and Vikash Kumar. Roboagent: Generalization and efficiency in robot manipulation via semantic augmentations and action chunking. In *2024 IEEE International Conference on Robotics and Automation (ICRA)*, pages 4788–4795. IEEE, 2024.

[5] Kevin Black, Noah Brown, Danny Driess, Adnan Esmail, Michael Equi, Chelsea Finn, Niccolo Fusai, Lachy Groom, Karol Hausman, Brian Ichter, et al. Pi0: A vision-language-action flow model for general robot control. *arXiv preprint arXiv:2410.24164*, 2024.

[6] Qingwen Bu, Jisong Cai, Li Chen, Xiuqi Cui, Yan Ding, Siyuan Feng, Shenyuan Gao, Xindong He, Xuan Hu, Xu Huang, et al. Agibot world colosseo: A large-scale manipulation platform for scalable and intelligent embodied systems. *arXiv preprint arXiv:2503.06669*, 2025.

[7] Remi Cadene, Simon Alibert, Alexander Soare, Quentin Gallouedec, Adil Zouitine, Steven Palma, Pepijn Kooijmans, Michel Aractingi, Mustafa Shukor, Dana Aubakirova, Martino Russi, Francesco Capuano, Caroline Pascal, Jade Choghari, Jess Moss, and Thomas Wolf. Lerobot: State-of-the-art machine learning for real-world robotics in pytorch. https://github.com/huggingface/lerobot, 2024.

[8] Tianxing Chen, Zanxin Chen, Baijun Chen, Zijian Cai, Yibin Liu, Zixuan Li, Qiwei Liang, Xianliang Lin, Yiheng Ge, Zhenyu Gu, et al. Robotwin 2.0: A scalable data generator and benchmark with strong domain randomization for robust bimanual robotic manipulation. *arXiv preprint arXiv:2506.18088*, 2025.

[9] Yuanpei Chen, Tianhao Wu, Shengjie Wang, Xidong Feng, Jiechuan Jiang, Zongqing Lu, Stephen McAleer, Hao Dong, Song-Chun Zhu, and Yaodong Yang. Towards human-level bimanual dexterous manipulation with reinforcement learning. *Advances in Neural Information Processing Systems*, 35:5150–5163, 2022.

[10] Cheng Chi, Zhenjia Xu, Siyuan Feng, Eric Cousineau, Yilun Du, Benjamin Burchfiel, Russ Tedrake, and Shuran Song. Diffusion policy: Visuomotor policy learning via action diffusion. *The International Journal of Robotics Research*, page 02783649241273668, 2023.

[11] Kourosh Darvish, Luigi Penco, Joao Ramos, Rafael Cisneros, Jerry Pratt, Eiichi Yoshida, Serena Ivaldi, and Daniele Pucci. Teleoperation of humanoid robots: A survey. *IEEE Transactions on Robotics*, 39(3):1706–1727, 2023.

[12] Sudeep Dasari, Frederik Ebert, Stephen Tian, Suraj Nair, Bernadette Bucher, Karl Schmeckpeper, Siddharth Singh, Sergey Levine, and Chelsea Finn. Robonet: Large-scale multi-robot learning. *arXiv preprint arXiv:1910.11215*, 2019.

[13] Frederik Ebert, Yanlai Yang, Karl Schmeckpeper, Bernadette Bucher, Georgios Georgakis, Kostas Daniilidis, Chelsea Finn, and Sergey Levine. Bridge data: Boosting generalization of robotic skills with cross-domain datasets. *arXiv preprint arXiv:2109.13396*, 2021.

[14] Wolfgang Echelmeyer, Alice Kirchheim, and Eckhard Wellbrock. Robotics-logistics: Challenges for automation of logistic processes. In *2008 IEEE International Conference on Automation and Logistics*, pages 2099–2103. IEEE, 2008.

[15] Hao-Shu Fang, Hongjie Fang, Zhenyu Tang, Jirong Liu, Chenxi Wang, Junbo Wang, Haoyi Zhu, and Cewu Lu. Rh20t: A comprehensive robotic dataset for learning diverse skills in one-shot. *arXiv preprint arXiv:2307.00595*, 2023.

[16] Galaxea. https://galaxea-ai.com/products/R1-Lite.

[17] Galbot. https://www.galbot.com/g1.

[18] Anna Henschel, Guy Laban, and Emily S Cross. What makes a robot social? a review of social robots from science fiction to a home or hospital near you. *Current Robotics Reports*, 2(1):9–19, 2021.

[19] Edward J Hu, Yelong Shen, Phillip Wallis, Zeyuan Allen-Zhu, Yuanzhi Li, Shean Wang, Lu Wang, Weizhu Chen, et al. Lora: Low-rank adaptation of large language models. *ICLR*, 1(2):3, 2022.

[20] Eric Jang, Alex Irpan, Mohi Khansari, Daniel Kappler, Frederik Ebert, Corey Lynch, Sergey Levine, and Chelsea Finn. Bc-z: Zero-shot task generalization with robotic imitation learning. In *Conference on Robot Learning*, pages 991–1002. PMLR, 2022.

[21] Yuheng Ji, Huajie Tan, Jiayu Shi, Xiaoshuai Hao, Yuan Zhang, Hengyuan Zhang, Pengwei Wang, Mengdi Zhao, Yao Mu, Pengju An, et al. Robobrain: A unified brain model for robotic manipulation from abstract to concrete. In *Proceedings of the Computer Vision and Pattern Recognition Conference*, pages 1724–1734, 2025.

[22] Tao Jiang, Tianyuan Yuan, Yicheng Liu, Chenhao Lu, Jianning Cui, Xiao Liu, Shuiqi Cheng, Jiyang Gao, Huazhe Xu, and Hang Zhao. Galaxea open-world dataset and g0 dual-system vla model. *arXiv preprint arXiv:2509.00576*, 2025.

[23] Dmitry Kalashnikov, Jacob Varley, Yevgen Chebotar, Benjamin Swanson, Rico Jonschkowski, Chelsea Finn, Sergey Levine, and Karol Hausman. Mt-opt: Continuous multi-task robotic reinforcement learning at scale. *arXiv preprint arXiv:2104.08212*, 2021.

[24] Alexander Khazatsky, Karl Pertsch, Suraj Nair, Ashwin Balakrishna, Sudeep Dasari, Siddharth Karamcheti, Soroush Nasiriany, Mohan Kumar Srirama, Lawrence Yunliang Chen, Kirsty Ellis, et al. Droid: A large-scale in-the-wild robot manipulation dataset. *arXiv*

preprint arXiv:2403.12945, 2024.

[25] Moo Jin Kim, Karl Pertsch, Siddharth Karamcheti, Ted Xiao, Ashwin Balakrishna, Suraj Nair, Rafael Rafailov, Ethan Foster, Grace Lam, Pannag Sanketi, et al. Openvla: An open-source vision-language-action model. *arXiv preprint arXiv:2406.09246*, 2024.

[26] Aixin Liu, Bei Feng, Bing Xue, Bingxuan Wang, Bochao Wu, Chengda Lu, Chenggang Zhao, Chengqi Deng, Chenyu Zhang, Chong Ruan, et al. Deepseek-v3 technical report. *arXiv preprint arXiv:2412.19437*, 2024.

[27] Bo Liu, Yifeng Zhu, Chongkai Gao, Yihao Feng, Qiang Liu, Yuke Zhu, and Peter Stone. Libero: Benchmarking knowledge transfer for lifelong robot learning. *Advances in Neural Information Processing Systems*, 36:44776–44791, 2023.

[28] Shilong Liu, Zhaoyang Zeng, Tianhe Ren, Feng Li, Hao Zhang, Jie Yang, Qing Jiang, Chunyuan Li, Jianwei Yang, Hang Su, et al. Grounding dino: Marrying dino with grounded pre-training for open-set object detection. In *European conference on computer vision*, pages 38–55. Springer, 2024.

[29] Songming Liu, Lingxuan Wu, Bangguo Li, Hengkai Tan, Huayu Chen, Zhengyi Wang, Ke Xu, Hang Su, and Jun Zhu. Rdt-1b: a diffusion foundation model for bimanual manipulation. *arXiv preprint arXiv:2410.07864*, 2024.

[30] Yueyue Liu, Zhijun Li, Huaping Liu, and Zhen Kan. Skill transfer learning for autonomous robots and human–robot cooperation: A survey. *Robotics and Autonomous Systems*, 128:103515, 2020.

[31] Steven Macenski, Tully Foote, Brian Gerkey, Chris Lalancette, and William Woodall. Robot operating system 2: Design, architecture, and uses in the wild. *Science Robotics*, 7(66):eabm6074, 2022. doi: 10.1126/scirobotics.abm6074. URL https://www.science.org/doi/abs/10.1126/scirobotics.abm6074.

[32] Oier Mees, Lukas Hermann, Erick Rosete-Beas, and Wolfram Burgard. Calvin: A benchmark for language-conditioned policy learning for long-horizon robot manipulation tasks. *IEEE Robotics and Automation Letters*, 7(3):7327–7334, 2022.

[33] Yao Mu, Tianxing Chen, Zanxin Chen, Shijia Peng, Zhiqian Lan, Zeyu Gao, Zhixuan Liang, Qiaojun Yu, Yude Zou, Mingkun Xu, et al. Robotwin: Dual-arm robot benchmark with generative digital twins. In *Proceedings of the Computer Vision and Pattern Recognition Conference*, pages 27649–27660, 2025.

[34] NVIDIA, Nikita Cherniadev Johan Bjorck andFernando Castañeda, Xingye Da, Runyu Ding, Linxi "Jim" Fan, Yu Fang, Dieter Fox, Fengyuan Hu, Spencer Huang, Joel Jang, Zhenyu Jiang, Jan Kautz, Kaushil Kundalia, Lawrence Lao, Zhiqi Li, Zongyu Lin, Kevin Lin, Guilin Liu, Edith Llontop, Loic Magne, Ajay Mandlekar, Avnish Narayan, Soroush Nasiriany, Scott Reed, You Liang Tan, Guanzhi Wang, Zu Wang, Jing Wang, Qi Wang, Jiannan Xiang, Yuqi Xie, Yinzhen Xu, Zhenjia Xu, Seonghyeon Ye, Zhiding Yu, Ao Zhang, Hao Zhang, Yizhou Zhao, Ruijie Zheng, and Yuke Zhu. GR00T N1: An open foundation model for generalist humanoid robots. In *ArXiv Preprint*, March 2025.

[35] NVIDIA, Nikita Cherniadev Johan Bjorck andFernando Castañeda, Xingye Da, Runyu Ding, Linxi "Jim" Fan, Yu Fang, Dieter Fox, Fengyuan Hu, Spencer Huang, Joel Jang, Zhenyu Jiang, Jan Kautz, Kaushil Kundalia, Lawrence Lao, Zhiqi Li, Zongyu Lin, Kevin Lin, Guilin Liu, Edith Llontop, Loic Magne, Ajay Mandlekar, Avnish Narayan, Soroush Nasiriany, Scott Reed, You Liang Tan, Guanzhi Wang, Zu Wang, Jing Wang, Qi Wang, Jiannan Xiang, Yuqi Xie, Yinzhen Xu, Zhenjia Xu, Seonghyeon Ye, Zhiding Yu, Ao Zhang, Hao Zhang, Yizhou Zhao, Ruijie Zheng, and Yuke Zhu. https://research.nvidia.com/labs/gear/gr00t-n1_5/, 2025.

[36] Abby O'Neill, Abdul Rehman, Abhiram Maddukuri, Abhishek Gupta, Abhishek Padalkar, Abraham Lee, Acorn Pooley, Agrim Gupta, Ajay Mandlekar, Ajinkya Jain, et al. Open x-embodiment: Robotic learning datasets and rt-x models: Open x-embodiment collaboration 0. In *2024 IEEE International Conference on Robotics and Automation (ICRA)*, pages 6892–6903. IEEE, 2024.

[37] Mikkel Rath Pedersen, Lazaros Nalpantidis, Rasmus Skovgaard Andersen, Casper Schou, Simon Bøgh, Volker Krüger, and Ole Madsen. Robot skills for manufacturing: From concept to industrial deployment. *Robotics and Computer-Integrated Manufacturing*, 37:282–291, 2016.

[38] Lerrel Pinto and Abhinav Gupta. Supersizing self-supervision: Learning to grasp from 50k tries and 700 robot hours. In *2016 IEEE international conference on robotics and automation (ICRA)*, pages 3406–3413. IEEE, 2016.

[39] Morgan Quigley, Ken Conley, Brian Gerkey, Josh Faust, Tully Foote, Jeremy Leibs, Rob Wheeler, Andrew Y Ng, et al. Ros: an open-source robot operating system. In *ICRA workshop on open source software*, volume 3, page 5. Kobe, 2009.

[40] Tianhe Ren, Qing Jiang, Shilong Liu, Zhaoyang Zeng, Wenlong Liu, Han Gao, Hongjie Huang, Zhengyu Ma, Xiaoke Jiang, Yihao Chen, et al. Grounding dino 1.5: Advance the" edge" of open-set object detection. *arXiv preprint arXiv:2405.10300*, 2024.

[41] Agilex Robotics. https://global.agilex.ai/products/cobot-magic, .

[42] AI2 Robotics. https://ai2robotics.com/, .

[43] Leju Robotics. https://www.lejurobot.cn/zh/application/kuavo-my, .

[44] Realman Robotics. https://realmanrobotics.com/, .

[45] Lin Shao, Toki Migimatsu, Qiang Zhang, Karen Yang, and Jeannette Bohg. Concept2robot: Learning manipulation concepts from instructions and human demonstrations. *The International Journal of Robotics Research*, 40(12-14):1419–1434, 2021.

[46] Lucy Xiaoyang Shi, Brian Ichter, Michael Equi, Liyiming Ke, Karl Pertsch, Quan Vuong, James Tanner,

Anna Walling, Haohuan Wang, Niccolo Fusai, et al. Hi robot: Open-ended instruction following with hierarchical vision-language-action models. *arXiv preprint arXiv:2502.19417*, 2025.

[47] BAAI RoboBrain Team. https://github.com/FlagOpen/RoboBrain-X0, 2025.

[48] Octo Model Team, Dibya Ghosh, Homer Walke, Karl Pertsch, Kevin Black, Oier Mees, Sudeep Dasari, Joey Hejna, Tobias Kreiman, Charles Xu, et al. Octo: An open-source generalist robot policy. *arXiv preprint arXiv:2405.12213*, 2024.

[49] TQ-Artisan. https://tqartisan.com/productDetails?type=A2.

[50] Unitree. https://www.unitree.com/g1/.

[51] Homer Rich Walke, Kevin Black, Tony Z Zhao, Quan Vuong, Chongyi Zheng, Philippe Hansen-Estruch, Andre Wang He, Vivek Myers, Moo Jin Kim, Max Du, et al. Bridgedata v2: A dataset for robot learning at scale. In *Conference on Robot Learning*, pages 1723–1736. PMLR, 2023.

[52] Liuyi Wang, Xinyuan Xia, Hui Zhao, Hanqing Wang, Tai Wang, Yilun Chen, Chengju Liu, Qijun Chen, and Jiangmiao Pang. Rethinking the embodied gap in vision-and-language navigation: A holistic study of physical and visual disparities. In *Proceedings of the IEEE/CVF International Conference on Computer Vision*, pages 9455–9465, 2025.

[53] Kun Wu, Chengkai Hou, Jiaming Liu, Zhengping Che, Xiaozhu Ju, Zhuqin Yang, Meng Li, Yinuo Zhao, Zhiyuan Xu, Guang Yang, et al. Robomind: Benchmark on multi-embodiment intelligence normative data for robot manipulation. *arXiv preprint arXiv:2412.13877*, 2024.

[54] Fan Xie, Alexander Chowdhury, M De Paolis Kaluza, Linfeng Zhao, Lawson Wong, and Rose Yu. Deep imitation learning for bimanual robotic manipulation. *Advances in neural information processing systems*, 33: 2327–2337, 2020.

[55] Han Xue, Jieji Ren, Wendi Chen, Gu Zhang, Yuan Fang, Guoying Gu, Huazhe Xu, and Cewu Lu. Reactive diffusion policy: Slow-fast visual-tactile policy learning for contact-rich manipulation. *arXiv preprint arXiv:2503.02881*, 2025.

[56] Jonathan Yang, Catherine Glossop, Arjun Bhorkar, Dhruv Shah, Quan Vuong, Chelsea Finn, Dorsa Sadigh, and Sergey Levine. Pushing the limits of cross-embodiment learning for manipulation and navigation. *arXiv preprint arXiv:2402.19432*, 2024.

[57] Tianhe Yu, Deirdre Quillen, Zhanpeng He, Ryan Julian, Karol Hausman, Chelsea Finn, and Sergey Levine. Meta-world: A benchmark and evaluation for multi-task and meta reinforcement learning. In *Conference on robot learning*, pages 1094–1100. PMLR, 2020.

[58] Wenyao Zhang, Hongsi Liu, Zekun Qi, Yunnan Wang, Xinqiang Yu, Jiazhao Zhang, Runpei Dong, Jiawei He, Fan Lu, He Wang, et al. Dreamvla: a vision-language-action model dreamed with comprehensive world knowledge. *arXiv preprint arXiv:2507.04447*, 2025.

[59] Tony Z Zhao, Vikash Kumar, Sergey Levine, and Chelsea Finn. Learning fine-grained bimanual manipulation with low-cost hardware. *arXiv preprint arXiv:2304.13705*, 2023.

[60] Wenshuai Zhao, Jorge Peña Queralta, and Tomi Westerlund. Sim-to-real transfer in deep reinforcement learning for robotics: a survey. In *2020 IEEE symposium series on computational intelligence (SSCI)*, pages 737–744. IEEE, 2020.

APPENDIX A
ACTION AND OBJECT TAXONOMY

To ensure standardized data collection, consistent annotation, and robust policy learning across diverse robotic platforms, we propose a unified and hierarchical taxonomy for robotic manipulation actions. The taxonomy is organized into 4 core categories based on *functional purpose, physical interaction type, and environmental effect*, each representing a distinct class of robot behaviors. The categories are defined as follows:

- **General Manipulation.** Basic low-level primitives that describe universal, frequently used robot motions, including grasping, placement, pushing, pulling, and alignment.
- **Object State Change.** Actions that alter the physical state, shape, or configuration of an object, such as pressing, folding, twisting, shaking, and tearing.
- **Object Relation Change.** Operations that modify the spatial or structural relationship between multiple objects, including stacking, insertion, assembly, attachment, and exchange.
- **Task-Specific Actions.** High-level specialized operations for domain-specific scenarios, including cleaning, cooking, pouring, cutting, device control, and writing.

To enhance language grounding and improve model robustness to linguistic variations, each action verb is accompanied by semantically consistent synonyms. These synonyms are used for textual data augmentation, enabling the model to better understand diverse natural language instructions and reduce annotation ambiguity. The complete glossary of standardized action verbs, synonyms, and formal definitions is presented in Table III, which serves as a foundational reference for data collection and annotation in the RoboCOIN dataset.

APPENDIX B
RTML SPECIFICATION

To formalize the constraints of robotic manipulation tasks in a structured and machine-interpretable manner, we design a **Robot Trajectory Markup Language (RTML)**, exemplified in Listing 1 for the "*pull bowl storage bread*" task. RTML adopts a hierarchical constraint architecture that decouples **Global Constraints** and **Local Constraints**, enabling modular specification of task-wide kinematic limits alongside stage-specific spatial-temporal and kinematic requirements.

For **Global Constraints**, RTML defines universal kinematic limits that apply to the entire task execution, including upper bounds for linear velocity (maximum: 0.5 m/s, mean maximum: 0.3 m/s) and linear acceleration (maximum: 12.0 m/s^2). These global constraints ensure basic safety and motion smoothness across all manipulation stages, preventing excessive kinematic values that may lead to mechanical instability or task failure.

For **Local Constraints**, RTML partitions the overall task into sequential, semantically meaningful subtasks *(e.g., `move_bowl_right`, `grasp_long_bread_left`, `place_long_bread_in_bowl`)*, each associated with a human-readable `match_subtask` description to align with natural language task definitions. Each stage specifies multi-dimensional constraints tailored to the subtask's requirements:

- **Workspace constraints** define the 3D Cartesian bounds for the active arm *(e.g., the right arm's workspace for moving the pink bowl is restricted to [0.10, -0.40, 0.10] to [0.25, -0.20, 0.30] in meters)*, ensuring the robot operates within task-relevant spatial regions.
- **Kinematic constraints** refine velocity limits *(e.g., linear velocity mean maximum of 0.10 m/s for bowl movement)* with additional statistical constraints *(e.g., standard deviation maximum of 0.08 m/s)* to control motion variability.
- **Idle arm constraints** impose strict velocity limits on the non-active arm *(e.g., left arm's linear velocity mean maximum of 0.05 m/s during right-arm bowl movement)* to avoid unintended motion interference.
- **Orientation constraints** *(e.g., angular mean deviation maximum of 0.8 rad and angular variance maximum of 0.15 for grasping long bread with the left arm)* regulate the pose stability of the end-effector for precise grasping.
- **Temporal constraints** define the minimum and maximum duration for each stage *(e.g., 2.0–8.0 seconds for bread grasping)* to ensure task execution efficiency and completeness.

By structuring RTML in this hierarchical manner, we enable clear delineation between overarching task constraints and stage-specific requirements, facilitating data quality control during trajectory collection and providing a robust framework for downstream robotic learning algorithms to interpret and adhere to task constraints.

APPENDIX C
ANNOTATION PIPELINE

To systematically annotate the multi-faceted aspects of robotic manipulation trajectories, we develop a comprehensive annotation pipeline consisting of three hierarchical pipelines: *Trajectory-Level Annotation, Segment-Level Annotation, and Frame-Level Annotation*, as illustrated in Figure 10.

Trajectory-Level Annotation Pipeline. As shown in Figure 10(a), trajectory-level annotation provides the semantic basis for understanding robotic manipulation scenes by converting raw visual observations into human-readable natural language descriptions, including the following two key steps:

1) **Object Detection.** A state-of-the-art detector (*e.g., Grounding DINO*) processes visual frames to detect and localize key objects, outputting structured class labels and normalized bounding box coordinates. The detector outputs structured information comprising object class labels and bounding box coordinates, formatted as numerical tuples that encapsulate the spatial distribution of each object (*e.g., [0.1,0.4,0.45,0.8] for a plate, [0.3,0.25,0.5,0.5] for a carrot*).
2) **Scene Description Generation.** This structured information is then passed to a large language model (*e.g., Deepseek R1*), which translates low-level spatial data

TABLE III: Robotic Manipulation Action Glossary

Category	Verb	Synonyms	Definition
General Manipulation	pick	grab, take, get	Grasp and lift an object from its position
	grasp	grip, clutch, hold	Firmly hold an object without positional change
	place	put, set, position	Put an object onto a surface or target location
	pass	hand over, give	Transfer an object between two hands/end-effectors
	rotate	twist, turn, revolve	Change the angular orientation of an object
	push	slide, shove	Move an object by applying forward force
	pull	drag, tug	Draw an object toward the agent
	lift	raise, hoist	Move an object upward to a higher position
	store	stow, deposit	Place an object inside a closed/semi-enclosed container
Object State Change	press	depress, push down	Apply continuous force to deform/activate an object
	click	tap, press briefly	Apply momentary force to actuate a button/switch
	open	unfold, unzip	Switch an object from closed to accessible state
	unzip	–	Open a zippered fastener
	unfold	spread out, expand	Flatten a folded or compact object
	close	shut, zip	Switch an object from open to closed state
	fold	tuck, collapse	Bend an object into a compact/layered form
	unscrew	loosen, twist off	Release a lid/cap by counterclockwise rotation
Object Relation Change	stack	pile, heap	Arrange objects vertically in layers
	arrange	line up, organize	Place objects in an orderly spatial pattern
	insert	put in, slot	Place one object into another structure
	plug in	connect, attach	Insert an electrical plug into a power socket
	remove	pull out, extract	Take an object out of a space/connection
	unplug	disconnect	Remove an electrical plug from a socket
	assemble	construct, build	Combine parts into a functional unit
	stick	paste, attach	Affix an object to a surface via adhesion
	swap	exchange, switch	Exchange positions of two objects
Task-Specific Actions	wipe	scrub, clean	Clean a surface via rubbing motion
	erase	remove marks	Eliminate traces or residues from a surface
	rinse	wash, flush	Clean an object using flowing water
	turn on	activate, start	Power on an electrical/mechanical device
	turn off	deactivate, stop	Power off an electrical/mechanical device
	pour	transfer, spill	Move liquid from one container to another
	scoop	ladle, dig out	Lift material using a spoon or scooping tool
	stir	mix, blend	Homogenize liquid/particulate matter
	cut	chop, slice, split	Separate an object using a sharp tool
	play	perform	Operate a musical instrument
	make	build, create	Construct an object or prepare food
	spell	recite letters	Form words by sequencing individual characters
	write	inscribe, jot	Produce characters on a surface

into coherent scene descriptions that summarize object positions, quantities, and spatial relationships, such as "*Two plates are placed at the middle-left and middle-right of the frame respectively; two radishes are arranged one above and one below beside the plates; two eggplants are at the bottom-right of the right plate.*"

By lifting raw visual detections to high-level semantics, this step builds a structured contextual representation for understanding robot actions and supports further analysis of manipulation tasks.

Segment-Level Annotation Pipeline. Figure 10(b) illustrates the segment-level annotation pipeline, which decomposes continuous robot manipulation trajectories into distinct action segments with fine-grained atomic sub-task labels. The core approach is to first detect key temporal points that partition the trajectory, then assign semantic labels to each resulting segment. Key temporal points for segment division are identified mainly based on robotic gripper states and task execution progress, including the following core types of temporal points:

- **Stationary state of the gripper.** This refers to the period when the gripper remains motionless during task execution, which usually indicates a transition between two consecutive atomic actions.
- **Gripper opening and closing transitions.** The moments corresponding to the "Open Gripper" and "Close Gripper" states serve as critical division points. For example, the moment the gripper starts to close marks the initiation of a grasping action, and the moment it starts to open indicates the initiation of a releasing action.
- **Task end moment.** The point when the robot completes all operations of a specific sub-task or the entire task.

Notably, there are other potential temporal points that could be considered for segment division, such as sudden changes in gripper velocity or acceleration, or significant shifts in object positions. After segmentation, each segment is labeled with a concise atomic sub-task description. By decomposing continuous behaviors into semantically meaningful segments, this step improves the interpretability of robot trajectories and supports fine-grained task analysis.

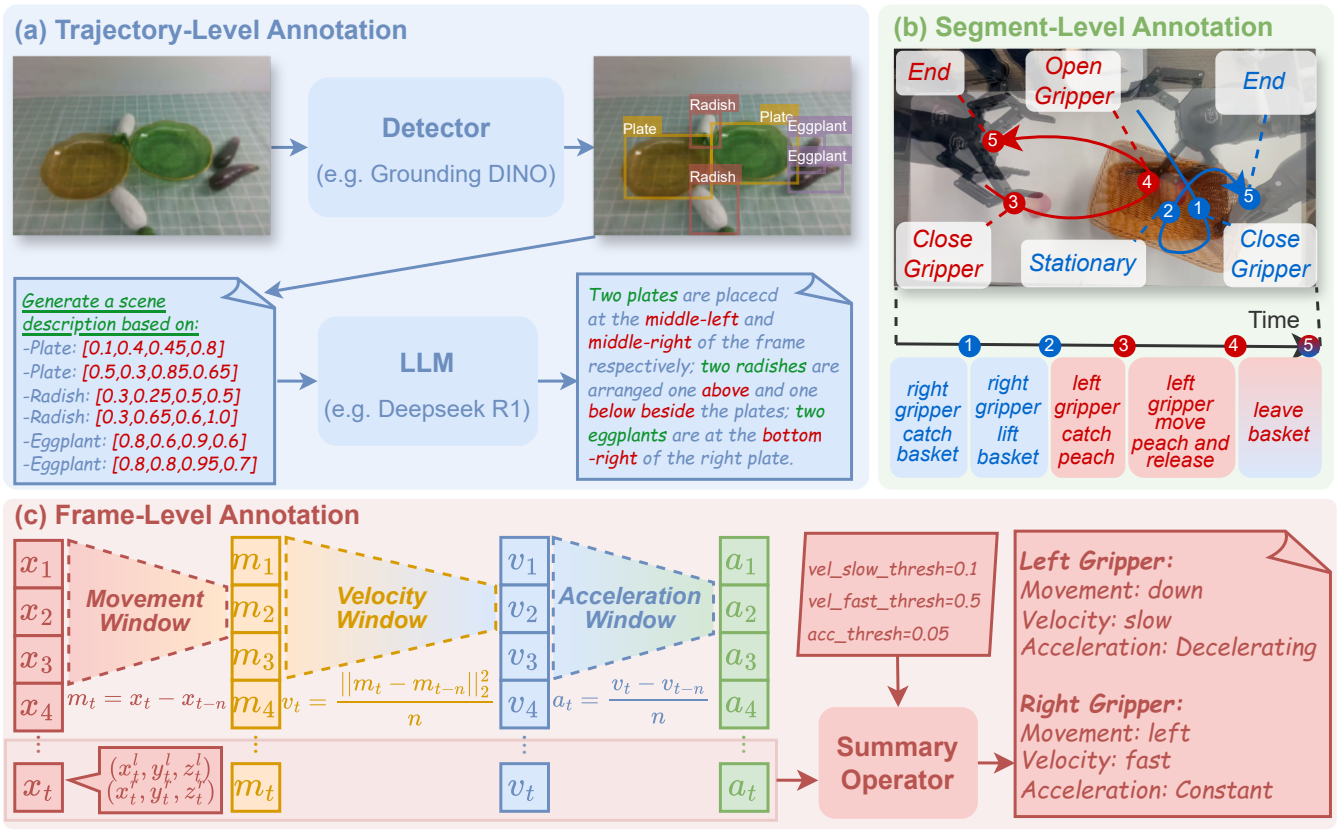


Fig. 10: **Annotation Pipeline Design.** (a) Trajectory-Level Annotation Pipeline. (b) Segment-Level Annotation Pipeline. (c) Frame-Level Annotation Pipeline.

Frame-Level Annotation Pipeline. Figure 10(c) presents the frame-level annotation pipeline, which extracts fine-grained gripper kinematics at each frame along manipulation trajectories. We use a cascaded window-based scheme to compute key motion metrics, as detailed below:

1) **Movement Window.** Computes the gripper displacement vector m_t as the coordinate difference between frame t and frame $t-n$:

$$m_t = x_t - x_{t-n},$$

2) **Velocity Window.** Estimates frame-wise velocity v_t from the L2 norm of consecutive displacement differences:

$$v_t = \frac{\|m_t - m_{t-1}\|_2}{n}.$$

3) **Acceleration Window.** Derives acceleration a_t as the normalized change in velocity:

$$a_t = \frac{v_t - v_{t-n}}{n}.$$

It should be emphasized that the cascaded window-based computation pipeline described below is a typical example for kinematic information extraction, and the specific implementation can be flexibly adjusted according to actual needs. This pipeline efficiently quantifies fine-grained gripper dynamics and supports robust trajectory quality assessment.

Summary Operator. After computing frame-level kinematic metrics including displacement, velocity, acceleration, and other motion features, a summary operator maps continuous numerical values to discrete gripper state labels via predefined thresholds. For example, given velocity threshold "vel_slow_thresh = 0.1" and "vel_fast_thresh = 0.5", the speed level is defined as follows:

$$\text{Vel} = \begin{cases} \text{Stationary}, & v < \text{vel\_slow\_thresh}, \\ \text{Slow}, & \text{vel\_slow\_thresh} \le v \le \text{vel\_fast\_thresh}, \\ \text{Fast}, & v > \text{vel\_fast\_thresh}. \end{cases}$$

The direction and acceleration level can be defined similarly with corresponding thresholds. Both grippers are processed in parallel, and the resulting discrete labels are combined to form a comprehensive motion description for each frame, encompassing multiple kinematic dimensions *(e.g. "Movement: down, Velocity: slow, Acceleration: Decelerating")*. Notably, the pipeline is fully customizable and users can extend it with additional windows *(e.g., jerk, angular velocity)* and reorder computation stages to fit task-specific needs across diverse manipulation scenarios. By organizing dense frame-wise kinematics into interpretable motion attributes, this pipeline enriches manipulation datasets with detailed motion priors, which are essential for robust policy learning and in-depth motion behavior analysis.

TABLE IV: Simulation task settings.

Task	Trajectories	Example Instruction
Blocks Ranking RGB	50	Arrange the red block, the green block, and the blue block from left to right in a row.
Grab Roller	50	Take hold of the roller using your arms.
Handover Block	50	Pass the red block from the left to the right.
Handover Mic	50	Pick the microphone and transfer it to the other arm.
Hanging Mug	50	Use the left arm to grab the mug, rotate it, set it down, then hang the mug onto the rack.
Lift Pot	50	Hold the pot firmly, then lift.
Place Bread Basket	50	Pick up the first bread and put it in the basket.
Place Bread Skillet	50	Grab the bread and place it inside the skillet.
Place Burger Fries	50	Use both arms to move the hamburg and the frenchfries to the tray.
Place Can Basket	50	Place the can in the basket and then lift the basket.
Place Can Plasticbox	50	Use both arms to move the left can and right can into the plasticbox.
Place Dual Shoes	50	Put two shoes, tips to the left, into the shoebox.
Put Object Cabinet	50	Open the cabinet's drawer and place the object inside it.
Stack Blocks Two	50	Shift the red block and the green block to the center and stack the green block on the red block.
Stack Bowls Two	50	Lift the first bowl, put it on the table, and stack the second bowl above.

TABLE V: Real-world task settings.

Task	Trajectories	Example Instruction
Block Basket	50	Put the block into the basket.
Peach Drawer	50	Put the peach in the drawer and close it.
Towel Basket	50	Put the towel into the basket.
Pass Bowl	50	Pass the bowl from the left to the right.
Peach Box	50	Open the box and put the peach in it.
Fold Towel	50	Fold the towel.
Grape Plate	298	Pick the grapes and place them on the plate.
Bread Bowl	997	Pick the bread and put it in the bowl.

Human Verification. To ensure annotation quality, we conduct human verification for both trajectory- and segment-level labels. Manual verification confirms that trajectory-level annotations achieve an overall accuracy of **84.2%**. The remaining errors include missed objects *(11.2%)*, localization errors *(4.4%)*, and redundant objects *(0.2%)*. For segment-level annotations, we use an online verification mechanism, where annotators check and adjust segment boundaries and action labels in real time to ensure consistency. Frame-level kinematic labels require no manual verification, as they are directly computed from accurate robot end-effector poses, ensuring numerical precision. This two-stage verification effectively yields reliable and consistent labels to support robust model training and cross-embodiment generalization in robotic manipulation.

APPENDIX D
EXPERIMENTAL TASK SETUPS

To evaluate the generalization and robustness of robotic manipulation algorithms across different environments, we design a dual-environment task setup comprising simulation and real-world tasks. Simulation tasks are tailored for cross embodiment transfer testing, while real-world tasks serve as the benchmark for evaluating hierarchical capability pyramid. The simulation environment comprises 16 distinct manipulation tasks, while the real-world environment includes 8 such tasks, each task is associated with 50 trajectories. Critically, these tasks are constructed with varying difficulty levels and a core focus on bimanual collaboration, covering a diverse range of manipulation paradigms for systematic evaluation.

Simulation Task Setups. As detailed in Table IV, the simulation task suite encompasses a wide variety of manipulation scenarios. The simulation tasks are implemented within the *RoboTwin 2.0* [8] virtual environment, where data collection is conducted using both *ARX-X5* and *Franka Emika Panda* dual-arm robots, both with an inter-arm distance of 0.8 meters. 50 trajectories are collected for each task, along with corresponding state information and natural language instructions. The simulation setup adopts a clean environment configuration without introducing background variations to ensure controlled evaluation; object deformation in simulation is limited, as most objects are rigid bodies, while deformable objects only feature a small number of movable joints *(e.g., drawer slides)*. Visual sequences for the simulation environment are presented in Figure 11 (a).

Real-World Task Setups. As shown in Table V, the real-world task suite includes a range of manipulation scenarios with varying object properties and collaboration requirements. The real-world tasks are executed on the *Realman RMC-AIDA-L* half-humanoid robot and the *Unitree G1edu-u3* humanoid robot. A total of 50 trajectories are collected for each of the 6 tasks in the hierarchical capability pyramid experiments, while 298 and 997 trajectories are gathered for the two respective tasks in the RTML experiments, along with corresponding state information and natural language instructions. Real-world experimental outcomes are inherently influenced by practical factors including the robot's control precision and ambient environmental noise, which introduces realistic variability and complexity absent in simulation. Task demonstrations for the real-world environment are shown in Figure 11 (b).

Out-of-Distribution Lighting Variations. To further enhance the robustness evaluation of manipulation algorithms under real-world visual variations, we introduce out-of-distribution (OOD) conditions during real-world task execution, and Figure 12 illustrates the lighting variations applied to the real-world task setup. This figure depicts three distinct lighting scenarios: *(Left) the original lighting, (Middle) strong lighting, and (Right) weak lighting*. These lighting variations introduce significant visual challenges, including uneven illumination,

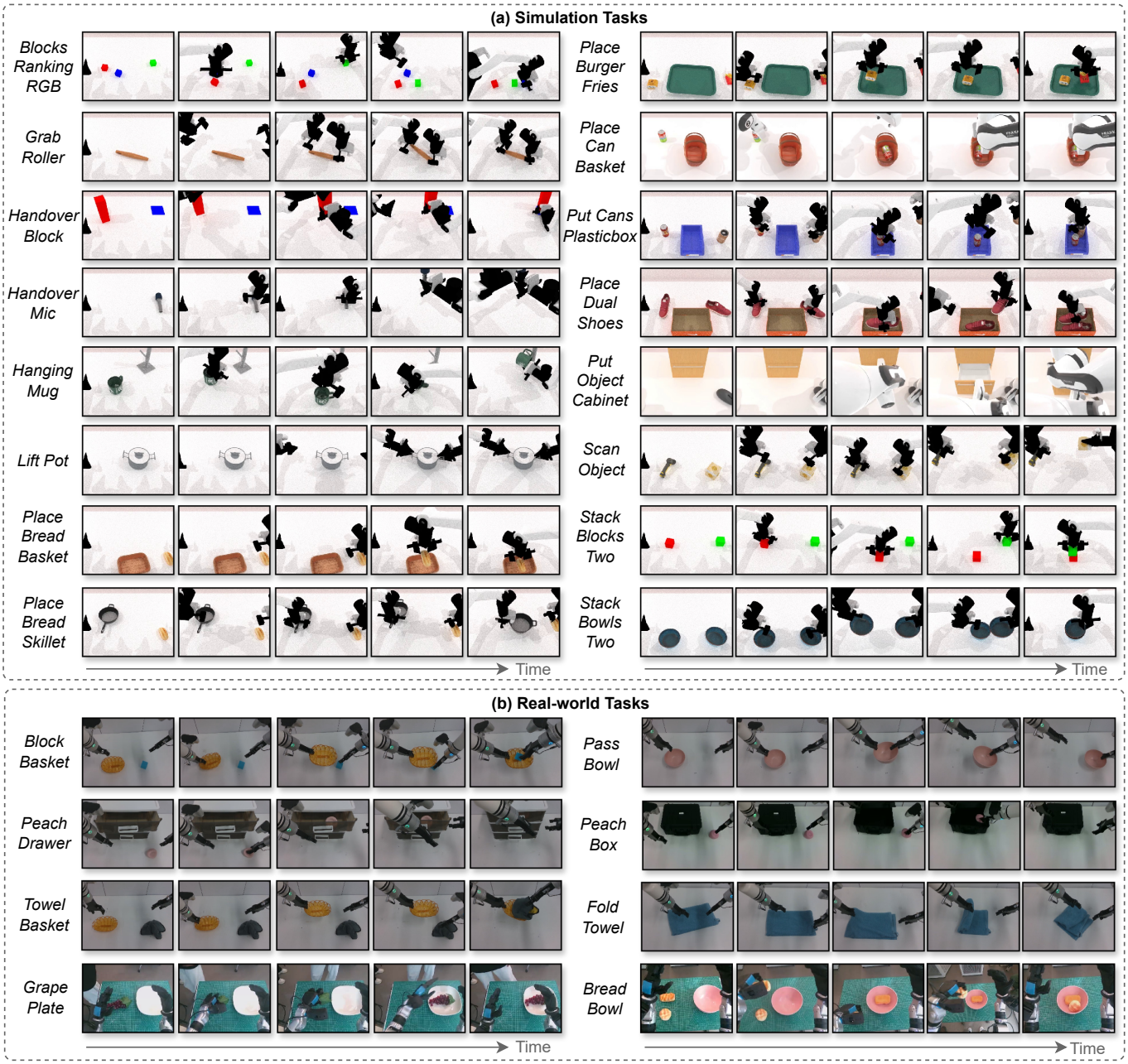


Fig. 11: **Example task setups** for (a) simulation environment, and (b) real-world environment.



Fig. 12: **Out-of-distribution lighting variations** in the real-world task setup, including *(Left)* original lighting, *(Middle)* strong lighting, and *(Right)* weak lighting.

cast shadows, reduced object texture visibility, and brightness disparities, which directly impact the performance of vision-based perception modules *(e.g., object detection, pose estimation)* critical for robotic manipulation. Notably, there are other OOD conditions in our real-world setup, such as object color changes and background variations. By incorporating such environment diversity into the real-world task setup, we ensure that the dataset and evaluation framework rigorously test the algorithm's ability to generalize across non-ideal conditions, which is essential for real-world deployment.

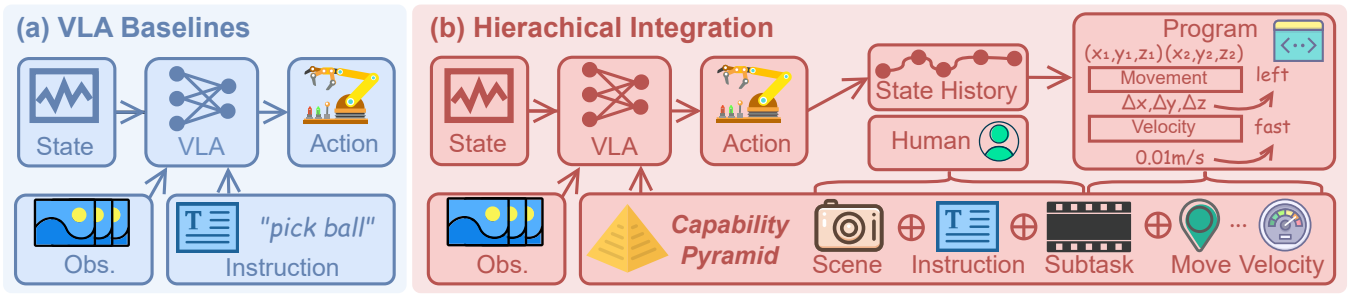


Fig. 13: **Hierarchical Capability Pyramid Integration.** (a) Vision-Language-Action (VLA) Baseline Model Implementation. The model directly maps multi-modal inputs (state, observation, instruction) to primitive actions without explicit hierarchical knowledge integration. (b) Hierarchical Integration Implementation. The framework incorporates hierarchical annotations into a structured decision-making pipeline, enhancing action generation with multi-level task knowledge and motion constraints.

APPENDIX E
HIERARCHICAL CAPABILITY PYRAMID INTEGRATION

Figure 13 illustrates the implementation framework of the proposed hierarchical annotation integration approach, alongside a baseline Vision-Language-Action (VLA) model for comparative analysis.

Vision-Language-Action Baseline Model. As depicted in 13 (a), the VLA baseline adheres to a standard end-to-end paradigm: it ingests raw state information, visual observations, and natural language instructions as multi-modal inputs, directly maps these modalities to robotic control signals via the VLA model, and outputs primitive manipulation actions. This approach relies solely on the model's learned representations to infer appropriate actions, without leveraging any explicit hierarchical task knowledge or motion constraints.

Hierarchical Integration. Figure 13 (b) presents the proposed framework, which augments the VLA pipeline by embedding hierarchical annotations into a structured decision-making pipeline. Our core objective is to validate the effectiveness of the hierarchical capability pyramid with a minimal, non-intrusive approach that can be seamlessly integrated into existing VLA models without altering their internal architecture or learned parameters. During inference, hierarchical task-action descriptions are constructed by fusing human instructions and an automated program module, with information derived at three complementary levels:

- **Trajectory-level information.** The overall trajectory structure is provided by human demonstrations, which defines the complete execution flow and high-level goal of the manipulation task.
- **Segment-level information.** Atomic subtask descriptions are predefined manually, consistent with the segment-level annotation pipeline introduced earlier. During inference, a rule-based program automatically identifies critical switching frames based on gripper states and task progress, enabling stable and smooth transitions between consecutive subtasks. More details on the switching point identification can be found in the **Segment-Level Annotation Pipeline in Appendix C**.
- **Frame-level information.** From historical pose sequences, the cascaded sliding-window scheme extracts instantaneous kinematics including displacement, velocity and acceleration. These continuous metrics are further converted into concise natural language motion descriptions via predefined thresholds, providing explicit, frame-wise constraints on movement direction, speed and acceleration trend. More details on the frame-level annotation process can be found in the **Frame-Level Annotation Pipeline in Appendix C**.

By integrating such multi-level hierarchical annotations, the framework injects structured task priors and fine-grained motion constraints into the input space of the VLA model, enabling it to generate actions that are both semantically consistent and kinematically feasible. We emphasize that this lightweight integration strategy serves primarily as a naive and proof-of-concept to verify the value of hierarchical priors, and we believe more effective integration methods can be explored in future work to further enhance the synergy between hierarchical knowledge and VLA models.

Listing 1: RTML Example ”pull bowl storage bread”

```yaml
# RTML V1.0
task:
  id: "pull_bowl_storage_bread"

  # Global constraints
  global_constraints:
    velocity:
      linear:
        max: 0.5            # m/s
        mean_max: 0.3       # m/s
    acceleration:
      linear:
        max: 12.0            # m/s2

  # Local stage constraints
  stages:
    - id: "move_bowl_right"
      match_subtask: "Move the pink bowl to the center of table with right hand"
      constraints:
        workspace:
          right:
            min: [0.10, -0.40, 0.10]
            max: [0.25, -0.20, 0.30]
        velocity:
          linear:
            mean_max: 0.10
            std_max: 0.08
        idle_arm:
          arm: "left"
          velocity_linear_mean_max: 0.05
        temporal:
          duration_min: 2.0
          duration_max: 6.0

    - id: "grasp_long_bread_left"
      match_subtask: "Grasp the long bread with left hand"
      constraints:
        workspace:
          left:
            min: [0.05, -0.05, -0.05]
            max: [0.25, 0.35, 0.20]
        orientation:
          left:
            angular_mean_deviation_max: 0.8
            std_max: [0.5, 0.5, 0.8]
            angular_variance_max: 0.15
        velocity:
          linear:
            mean_max: 0.12
            std_max: 0.10
        idle_arm:
          arm: "right"
          velocity_linear_mean_max: 0.05
        temporal:
          duration_min: 2.0
          duration_max: 8.0

    - id: "place_long_bread_in_bowl"
      match_subtask: "Place the long bread in pink bowl with left hand"
      constraints:
        workspace:
          left:
            min: [0.05, -0.05, -0.05]
            max: [0.25, 0.35, 0.20]
        velocity:
          linear:
            mean_max: 0.15
            std_max: 0.15
        idle_arm:
          arm: "right"
          velocity_linear_mean_max: 0.05
        temporal:
```

```yaml
      duration_min: 1.0
      duration_max: 4.0

  - id: "grasp_round_bread_left"
    match_subtask: "Grasp the round bread with left hand"
    constraints:
      workspace:
        left:
          min: [0.05, 0.00, -0.05]
          max: [0.25, 0.35, 0.20]
      orientation:
        left:
          angular_mean_deviation_max: 0.5
          std_max: [0.5, 0.5, 0.5]
          angular_variance_max: 0.15
      velocity:
        linear:
          mean_max: 0.12
          std_max: 0.10
      idle_arm:
        arm: "right"
        velocity_linear_mean_max: 0.05
      temporal:
        duration_min: 2.0
        duration_max: 8.0

  - id: "place_round_bread_in_bowl"
    match_subtask: "Place the round bread in pink bowl with left hand"
    constraints:
      workspace:
        left:
          min: [0.05, 0.00, -0.05]
          max: [0.25, 0.35, 0.20]
      velocity:
        linear:
          mean_max: 0.15
          std_max: 0.15
      idle_arm:
        arm: "right"
        velocity_linear_mean_max: 0.05
      temporal:
        duration_min: 1.0
        duration_max: 4.0

  - id: "End"
    match_subtask: "End"
    constraints:
      velocity:
        linear:
          mean_max: 0.12
          std_max: 0.12
      temporal:
        duration_max: 6.0
```